The United Nations University

GEOTHERMAL TRAINING PROGRAMME
Orkustofnun, Grensásvegur 9,
IS-108 Reykjavík, Iceland

Reports 2006
Number 14

MAINTENANCE CHALLENGES IN THE OPERATION OF A GEOTHERMAL POWER STATION: A CASE FOR OLKARIA II PLANT - KENYA

Johnson W. Ndege
Kenya Electricity Generating Company Ltd.
Olkaria Geothermal Power Plant
P.O Box 785, Naivasha 20117
KENYA
jndege@kengen.co.ke

ABSTRACT

The performance status of a power plant and its generating equipment can be determined by monitoring their running parameters. This is carried out by recording the individual equipment operating parameters from various instruments e.g. turbine inlet pressure, steam flowrate, steam chest pressure, etc. in logs and computer back-ups of the same, and by analyzing the data obtained to determine power plant performance.

Operation of Olkaria II power plant was started in the year 2002, with Unit I turbine taking steam at a flowrate of 69.4. After operating for 2 years, steam chest pressure increased from 3.5 bar-a to 4.1 bar-a and steam consumption increased to 72.2 kg/s, with the turbine power generation capacity at 34.3 MWe out of rated 35.0 MWe. After dismantling and inspecting the turbine and its major auxiliary equipment, it was found that significant sulphur deposition and scaling and related compounds had occurred on the turbine shroud, the gas cooler and the cooling tower, reducing their efficiency and leading to reduced power.

The main non-condensable gases in steam at Olkaria II are CO_2 and H_2S (0.75% of steam by weight). Sulphur is formed by partial oxidation of H_2S and scaling occurs from solutes in brine carried over to steam pipelines due to inefficient separation. Constant inspection/maintenance and good operating practices have proved to be useful in restoring the plant to its optimal operating condition. On the other hand, corrosion and erosion of the turbine blades have been a major challenge in the operation of the plant.

1. INTRODUCTION

Access to energy is fundamental to our civilisation, and our economic and social development fuels a growing demand for reliable, affordable and clean energy. Moreover, nearly 1.6 billion people, or roughly a quarter of the world's population, need access to modern energy services (World Energy Council, 2004). However, recent events, including increasing tensions in oil-rich nations and the

resulting price volatilities, evolving energy regulations, environmental legislation and diminishing resources call for a balanced energy mix, and maximum effort in the efficient use of available resources. This involves understanding the energy resources, energy generation processes and facilities, and laying down elaborate maintenance strategies for their performance improvement and maximum resource utilization.

Maintenance is one of the powerful tools used by practicing engineers to rehabilitate engineering facilities to improve their performance. It involves a good understanding of the equipment and its operations and also the energy degrading processes. Good visual inspection and analysis of operating parameters are good indicators of equipment performance status. Further, equipment dismantling to access internal parts and correction of defects/non-performing processes is equally important. Before dismantling, a detailed analysis of measured values and a comparison with design parameters is done, clearly showing processes which degrade with time.

In this report, the processes and power generating facilities of Olkaria II power plant in Kenya are discussed. Analysis of measured parameters and the main maintenance set-backs and experience are enumerated. The maintenance procedures undertaken to solve them are presented. Suggestions to prevent the recurrence or on-set of the same problems are presented. These set-backs are also experienced in turbines in the Olkaria I power plant, which lead to operations at lower plant load conditions.

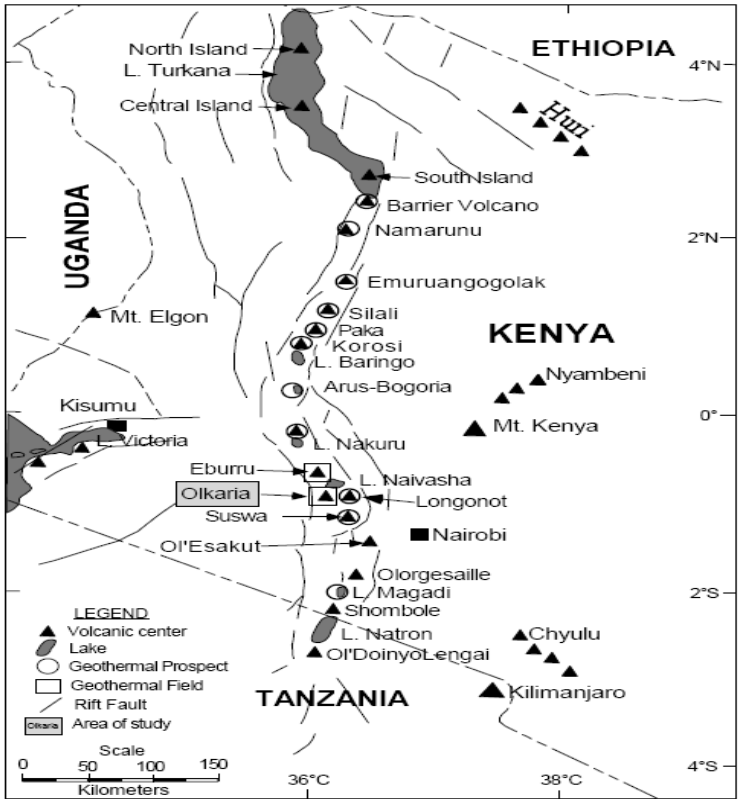

FIGURE 1: Map of Kenya showing the location of Olkaria geothermal area (Lagat, 2004)

Olkaria II power plant is located within the Greater Olkaria geothermal area in the Kenyan rift, which is about 120 km northwest of Nairobi (Figure 1). The plant has 2×35 MWe direct-contact steam condensing turbines driving power generators. The first turbine was commissioned in August 2002, followed by a second in November of the same year. The 2 turbines receive steam from 20 production wells in Olkaria Northeast geothermal field located in the Olkaria geothermal area. Four hot re-injection and two cold re-injection wells receive hot separated brine and cold condensate, respectively. The resource is characterised with hot springs and volcanic complexes, which consist of rhyolite domes and ashes, the youngest of which was dated as about 200 years old (Clarke et al., 1990).

Normally, during power plant operation, measured parameters are recorded manually and others are backed-up in computers for easy recall. Individual equipment and process logs are also used to evaluate equipment and plant status. Also, other performance indicators e.g. equipment and plant *availability factors*, *load factors*, *utilisation factors*, and *frequency of breakdowns* (see literature review) are used to estimate the overall plant status. While these measures give a good indication of machine and plant status, they fail to qualify and quantify maintenance problems unless a turbine is opened to access internal parts.

Geothermal resources are finite and renewable (World Energy Council, 2004), requiring continuous monitoring for resource assessment, utilisation, performance improvement and sustainable use. For example, at Olkaria I power plant, the field draw-down (Olkaria East field), after the commissioning of an extra turbine in 1985, led to the generation of only 30 MWe out of an installed capacity of 45 MWe (Ofwona, 2002). Extra wells were drilled to make up the steam deficit and to restore production to the installed capacity. If field monitoring had been effective and machine efficiencies maintained to their optimum, the rate of steam decline could have been lessened.

In this report, the operating process of the Olkaria II plant is simplified into sub-systems and main equipment. The operation of major equipment in each sub-system is discussed and parameters analysed, a visual inspection was conducted and interpretations made. Maintenance work undertaken on various equipment to improve degrading and in-efficient processes is then presented, discussed and suggestions made. Since reservoir fluid from the resource is the major contributor to almost all maintenance problems, its chemistry is also discussed in detail.

2. LITERATURE REVIEW

Olkaria II power station receives steam from Olkaria Northeast field which measures about 6 km^2 in area. The field has 20 production wells, 4 hot re-injection wells and 2 cold re-injection wells. In addition to the deep wells, 3 shallow wells, M1, M2 and M3 were drilled as field monitoring wells but are not currently in use. Further, the field has been divided into eastern and western fields for better operation and management.

The well casing programme consists of 20'' diameter surface casing; 13 3/8'' anchor casing; 9 5/8'' production casing, and 7'' slotted liners. The production casing usually extends to between 600 and 900 m depth while the drilled well depth ranges from 1800 to 2500 m.

2.1 Fluids chemistry

The chemistry of well discharges usually varies from one field to another. It also varies from one well to another, within the same field. After sampling and analysis of different wells fluids, mean values of well chemistry are taken to be representative of reservoir fluids. Deep reservoir fluid chemistry is influenced by boiling processes, fluid-rock interactions and mixing processes.

Chemical components in geothermal fluids are grouped into 2 distinct categories: mineral forming components; and conservative components. Mineral forming components: SiO_2, Na, K, Ca, Mg, S-H_2S and SO_4, C-CO_2, F, Al, Fe, Mn, etc. give information on deep reservoir temperatures, and boiling and mixing processes. Conservative components, e.g. Cl, B, and stable isotopes of deuterium and oxygen, are useful in determining reservoir recharge and re-injection (Wambugu, 1996).

Olkaria Northeast field wells discharge sodium-chloride water, with an average pH of about 6.7 to 7.4. The concentrations of sodium range from 450 to 850 ppm; chlorides range from 500 to 900 ppm (Appendix I); and water may be considered dilute with total dissolved solids (TDS) of about 2,500 ppm (Wambugu, 1996). The total carbonate concentration in the reservoir, calculated as CO_2, ranges from 1,000 to 2,000 ppm in most well fluids.

After separation of reservoir water into brine and steam, most of the non-condensable gases (NCGs) escape into the gaseous phase (steam) while other gases remain in the liquid phase. Also, depending on separation efficiency, some chemicals with principal species being Na, K, Cl, Ca, Fe, etc. are mechanically carried over into the steam supply. Other chemicals with appreciable solubility in steam at the separator temperature (150°C) will partition into steam as molecular species and thus cannot be

removed by mechanical separation. These consists of CO_2, H_2S, H_2, N_2, CH_4, silica (SiO_2), B, F, As, etc. The concentrations of chemicals in steam phase for Olkaria Northeast field were analysed and are given in Table 1 below.

The cyclone separators are vertical cylinders and are designed for high-efficiency steam separation (dryness fraction of 99.98%), so as to minimise the impurities in steam. Also, due to the relatively high percentage of non-condensable gases in the steam, the condensate formed has a pH of about 3.5.

TABLE 1: Chemical compositions of the steam phase for Olkaria Northeast field

Item	Description	Unit	Value
Impurities in steam	Na	mg/kg	0.5
	K	mg/kg	0.5
	Cl	mg/kg	1.0
	Fe	mg/kg	1.0
	SiO_2	mg/kg	0.5
Non-condensable gases (NCGs)	NCGs in steam	weight %	0.75
Composition of gases in NCGs	CO_2	weight %	94.6
	H_2S	weight %	2.6
	H_2	weight %	1.6
	N_2	weight %	0.9
	CH_4	weight %	0.3

2.1.1 Scaling

Scaling is a common phenomenon in all geothermal installations in the world. It occurs due to interaction of geothermal water with rocks and boiling processes deep in the reservoir, resulting in supersaturated water due to the dissolution of minerals. Dissolution may be accelerated by temperature and, sometimes, it may be retrogressive depending on the solute (Gunnarsson et al., 2005). Calcite, silica and metal pyrite deposition are the most common scales sited in Olkaria Northeast field.

Calcite scaling is largely confined to wet wells and occurs when geothermal water becomes supersaturated with calcite due to a decrease in partial pressure of carbon dioxide leading to its precipitation. It occurs in both low- and high-temperature geothermal installations as polymorphs of calcium carbonate which include vaterite and aragonite (Opondo, 2002). Calcite deposition is highly controlled by water temperature and pH, according to the equation:

$$Ca^{2+}{}_{(aq)} + 2HCO^{-}{}_{3\,(aq)} = CaCO_{3(s)}\,(Calcite) + CO_2 + H_2O \quad (1)$$

The solubility of silica in geothermal fluid is very dependent on temperature, the initial degree of super-saturation, salinity, pH, and the presence (or absence) of colloidal particles. Thus, separation temperatures of geothermal fluid need to be carefully chosen so that much of the silica will remain in solution or allow it to come out of solution before injection. Silica is mainly deposited as quartz or amorphous silica. Quartz (controls solubility of hot reservoir fluid) is deposited in the temperature range of 100-250°C and amorphous silica (controls solubility of low temperature fluid) in the range of 7-250°C (Gunnarsson, et al., 2005; Dipippo, 2005) depending on saturation, according to the equation:

$$OFeOH\,.\,H_2O + Si(OH)_4 = Fe(OH)_3\,.\,SiO_{2(s)} + 2H_2O \quad (2)$$

Metal sulphides, silicates and oxides are also common scaling problems in many low- and high-enthalpy geothermal installations. In low-enthalpy fluids containing high concentrations of dissolved solids, severe corrosion of mild steel production well casings occur. The iron oxides formed from this

corrosion react rapidly with sulphide-rich geothermal fluids causing metal sulphide deposition, mainly found in high-temperature environments. Iron sulphides identified in production and re-injection wells are pyrite, mackinawite, pyrrhotite and small amounts of iron and calcium carbonates (Lichti and Braithwaite, 1980).

In high-enthalpy systems, metal sulphides and oxides are also deposited in surface equipment e.g. separators, silencers, and weir boxes, etc. due to cooling and pH change accompanying flashing processes leading to the concentration of metal ions.

2.1.2 Corrosion

Corrosion is an enormous challenge in both low- and high-temperature geothermal installations. It is most prevalent in wellhead equipment, transmission pipelines and geothermal fluid utilisation facilities. Also, re-injection wells, power plant substations, and electronic devices used to control utilisation processes, etc. are attacked by corrosion leading to their degradation and inefficiency.

The most common forms of corrosion encountered in both low- and high-temperature geothermal installations are general corrosion, pitting corrosion, crevice corrosion, turbulence corrosion, galvanic corrosion, selective attack and stress corrosion cracking. All these forms of corrosion are accelerated by the presence of oxygen, high pH, high temperature, and the presence of water or moist air, characteristic of geothermal fluid (Gunnarsson et al., 2005). Corrosion is well explained by the anode/cathode reactions below. Since most installations are made of mild steel and iron alloys, the anodic/cathodic reactions are given with iron attack in mind.

Cathode reaction:

$$4e^- + O_2 + 2H_2O = 4OH^-_{(aq)} \quad (3)$$

Anode reaction for iron:

$$2Fe = Fe^{2+}_{(aq)} + 4e^- \quad (4)$$

Combining these two reactions to form a *total reaction:*

$$2Fe + O_2 + 2H_2O = 2Fe(OH)_{2(s)} \quad (5a)$$

$$2Fe(OH)_2 + ½\, O_2 + H_2O = 2Fe(OH)_{3(s)}\ (rust) \quad (5b)$$

Various methods are employed to prevent corrosion attacks: good material selection; minimising oxygen ingress by painting; the use of fibre glass and stainless steel material; lagging; pH control; and good design among others.

2.2 Turbine

The turbine is the most important and costly equipment in a geothermal power plant, though it depends on size, construction and the power cycle. Steam can be admitted into a turbine as: direct dry single-pressure steam; separated single-pressure steam; single-flash single-pressure steam; double-flash 2-pressure steam; or multi-flash (3 or more pressures). Other possible power cycles are brine/hydrocarbon binary cycle; or as hybrid fossil systems, among others.

After steam is expanded through a turbine, it is exhausted into the atmosphere (back pressure turbine) or condensed into a condenser (condensing exhaust turbine). In binary plants, geothermal fluid heats a secondary fluid in a heat exchanger, and the secondary fluid is expanded through a turbine (Organic Rankine Cycle). In hybrid systems, geothermal fluid is used to preheat a working fluid, then flue gases from coal or fossil oil superheats the working fluid.

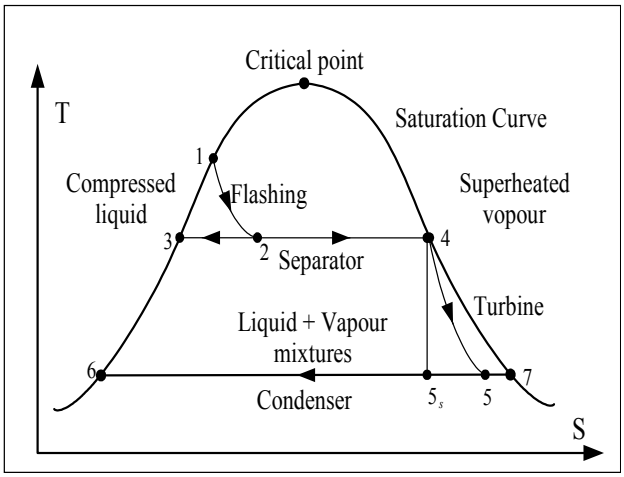

FIGURE 2: T-S diagram for a single-flash plant showing expansion in turbine

For separated single-flash steam, Figure 2 (T-S diagram) shows geothermal fluid from a production well at 1, passing into a cyclone separator at 2, where it is separated into liquid (brine), 3, and a steam phase at 4. Steam expands through the turbine and is exhausted into the condenser. The energy of inlet steam (inlet enthalpy), h_4, is reduced to thermal and pressure energy (exit enthalpy), h_{5s}, at exhaust conditions. Under isentropic expansion (constant entropy), point 4 to 5s, the work extracted from a steam flowrate of 1 kg/s is given as:

$$W = h_4 - h_{5s} \tag{6}$$

where W = Work output from turbine (kJ/kg);
h_4 = Steam inlet enthalpy (kJ/kg);
h_{5s} = Steam exit enthalpy (kJ/kg).

However, isentropic expansion is an ideal process and the factor, isentropic efficiency, η, is introduced to compare the actual turbine expansion to the isentropic expansion process, given by the formula below:

$$\eta = \frac{Actual\ Expansion}{IsentropicExpansion} = \frac{h_4 - h_5}{h_4 - h_{5s}} \tag{7}$$

where h_5 = Actual steam exit enthalpy after expansion (kJ/kg).

For steam flowrate, $\dot{m}$ (kg/s), actual work extracted from the turbine, is given by:

$$P_{actual} = \dot{m}(h_4 - h_5) \tag{8}$$

where P_{actual} = Turbine power output (kW).

To extract maximum energy from the turbine, steam is expanded until it is at as low a pressure as possible. However, the limiting conditions are the exhaust dryness fraction (X > 86%), and the cooling water temperature which depends on ambient conditions.

Another factor which is important in a power plant is the utilization efficiency, η_u, which compares the turbine output with the maximum theoretical obtainable output when steam is exhausted to sink conditions and is given by:

$$\eta_u = \frac{Power\ output}{Exergy} \tag{9}$$

In power generation practice, some terms used are defined below:

Availability facto is the ratio of the time the turbine is running to the total available time;
Load factor is the ratio of the units of power generated to the power that the turbine could have generated, if it was running at the rated output for the total available time;
Utilisation factor is the ratio of units of power generated to the power that the turbine could have generated, if it was running at the rated output for the actual time run;
Frequency of breakdowns is the number of times the turbine trips in a specific time e.g. a month.

2.3 Condenser

In geothermal power plants, condensers are used to condense turbine exhaust steam, hence creating sub-atmospheric conditions in the condenser. Back pressure turbines do not use condensers, instead exhausting the steam directly to the atmosphere.

Condensers are mainly divided into two types: surface condensers and direct-contact condensers (spray, barometric and jet types). In surface condensers, turbine exhaust steam passes through the outer surface of a bank of tubes carrying cold water, hence condensing steam on the shell side. In direct-contact condensers, exhaust steam is directly sprayed with cold water (mixing two streams), with the subsequent steam and gas cooling and condensation. In barometric condensers, cooling water is made to cascade down through a series of baffles and thoroughly mixes with turbine exhaust that is rising from a lower inlet. In jet condensers, exhaust steam and cooling water are made to cascade down to a diffuser, (El-Wakil, 1984).

Condensers are designed to provide low turbine exhaust pressures for maximum turbine efficiency and work extraction, and to ensure minimum cooling water for complete steam condensation and the reduction of dissolved geothermal gases. In order to meet these requirements, some features are included in the condensers design:

- Minimum pressure drop for both steam/gas and cooling water distribution system;
- Maximum removal of non-condensable gases;
- High heat transfer coefficients for maximum steam condensation and gas cooling;
- Prevention of ambient air leakages; and
- Compactness and low water level arrangement.

The design of a direct-contact condenser is determined by the total volume required for maximum heat and mass transfer. The heat transfer is calculated by the empirical formulae:

$$V = \frac{Q}{UadT} \tag{10}$$

where V = Volume of condenser (m^3);
Q = Condenser heat load (W);
U = Overall heat transfer coefficient ($W/m^2 K$);
a = Internal area (volumetric term for indeterminate transfer area of drops) (m^2/m^3);
dT = Logarithmic mean temperature difference (K).

However, manufacturers generally use the heat transfer methods with modifications of these empirical relationships.

The condensation process occurs when the latent heat of the inlet steam at point 1 (Figure 3) is absorbed as sensible heat in the cooling water at point 2. When the temperature of the water is high enough to reverse the gas absorption, the stripping process is said to occur. This occurs when the turbine exit steam has high water vapour content such that the partial pressure of gas is lower than the

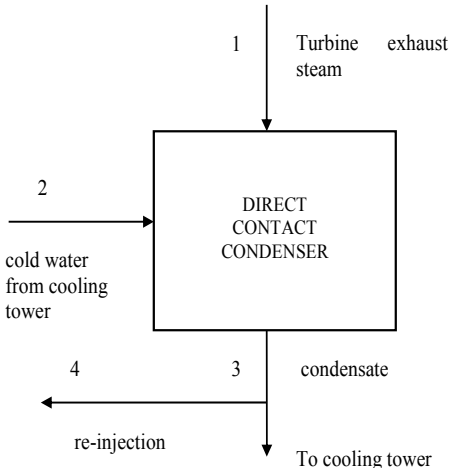

FIGURE 3: Turbine exhaust steam and water streams in condenser

equilibrium partial pressure and the gas tends to be stripped from the liquid (Hart, 1979). The mass and energy balance, with $\dot{m}$ and h denoting mass-flow rates and specific enthalpies, respectively, give:

$$\dot{m}_1 = \dot{m}_4 \quad \text{and} \quad \dot{m}_1 + \dot{m}_2 = \dot{m}_3 \qquad (11)$$

$$\dot{m}_1 h_1 + \dot{m}_2 h_2 = \dot{m}_3 h_3 \qquad (12)$$

The condenser has to operate in the stripping regime, such that 95% of the steam is condensed in the main condenser, and provide a gas cooler to operate in the absorption regime to complete condensation and gas cooling. The two streams, one with a large flow of condensate from the main condenser with a low concentration of dissolved gases, and a smaller one from the gas cooler containing highly dissolved gases, are mixed to form one stream at 3, with acceptably low gas content.

2.4 Cooling tower

Turbine exhaust steam carries a lot of heat which requires dissipation. The heat rejection process can be be done using several different methods dependent on the cooling medium: cooling ponds/lakes; spray ponds/canals; '*once-through*' cooling; or the use of cooling towers (wet mechanical draft, wet natural draft, dry/wet cooling towers) among others.

Most cooling towers use evaporative cooling, where about 1-3% of re-circulating water evaporates to cool the remainder of the stream by 8-12°C (evaporative cooling), depending on the ambient wet and dry-bulb temperature. Water to be cooled is brought into intimate contact with a moving air stream. About 75% of the cooling takes place by evaporation and the remainder by conduction to raise the dry bulb temperature of the air. The air stream leaves the top of the tower, when it is at near-saturation condition, as a plume.

To enhance heat exchange between water and air, the area of contact between the water and air stream is increased by spraying water in thin jets into packing fills to form thin water film.

2.4.1 Energy and mass balance in a wet cooling tower

For a better understanding of a wet cooling tower, some terms needs to be defined:

Relative humidity, φ, is the ratio of partial pressure of water vapour, P_v, in air to the partial pressure of water vapour that would saturate the air at its temperature, P_{sat}:

$$\varphi = \frac{P_v}{P_{sat}} \qquad (13)$$

Humidity ratio, $\acute{\omega}$, is the mass of water vapour per unit mass of dry air:

$$\omega = \frac{m_v}{m_a} = \frac{0.622 P_v}{P - P_v} \tag{14}$$

where P = Atmospheric pressure.

Wet-bulb temperature, T_{wb} is the temperature of air when it is fully saturated with water vapour;
Dry-bulb temperature, T_{db} is the temperature of air as commonly measured i.e. when not fully saturated with water vapour;
Approach is the difference in temperature between the cold water entering the cooling tower and the wet-bulb temperature of the outside air;
Range is the temperature difference between cold water exiting tower, and hot water entering the cooling tower.

The energy and mass balance between the hot water and cold air stream entering the cooling tower, and the cold water and hot/moist air streams exiting the tower, can be summarised by considering the tower as a control volume (Figure 4). By neglecting changes in kinetic and potential energies, assuming no heat and work transfer takes place across boundaries, denoting subscripts 1 and 2 to refer to air inlet and exit of tower, and *A* and *B* as circulating water inlet and exit of tower (El-Wakil, 1984), respectively, we get the following relationships:

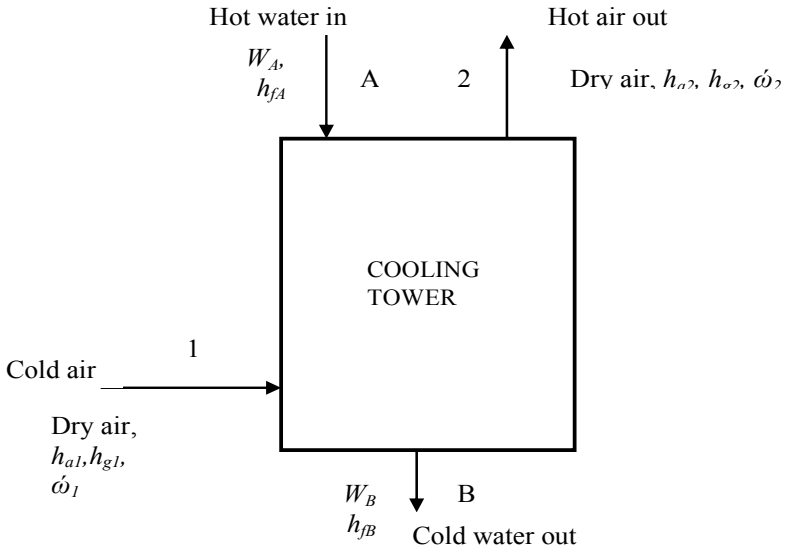

FIGURE 4: Cooling tower water and air streams balance)

Energy and mass in

$$M_i = h_{a1} + \omega_1 h_{g1} + W_A h_{WA} \tag{15}$$

Energy and mass out

$$M_o = h_{a2} + \omega_2 h_{g2} + W_B h_{WB} \tag{16}$$

where h_{a1}, h_{a2} = Enthalpy of cold air at tower inlet and outlet, respectively (kJ/kg);
ω_1, ω_2 = Humidity ratio of air at inlet and outlet, respectively;
h_{g1}, h_{g2} = Enthalpy of vapour in air at inlet and outlet of tower, respectively (kJ/kg);
W_A, W_B = Circulating water flowrate at inlet and outlet, respectively (kg/s);
h_{WA}, h_{WB} = Enthalpy of circulating water at inlet and outlet, respectively (kJ/kg).

The energy and mass entering the tower is equal to the energy and mass exiting the tower. Thus unknown values can be calculated.

2.5 Pumps

2.5.1 Introduction

In order to make water and other liquids move in pipes and channels, mechanical energy is usually imparted by pumps. Pumps operate like fans, though fans normally deal with air and gases. They are mostly driven by being coupled directly to the motor driving shaft or through some speed reduction devices like gear wheels.

2.5.2 Classification of pumps

Pump types can be grouped into two main categories: centrifugal (dynamic) and positive displacement pumps. Centrifugal pumps impart kinetic energy to a liquid by the spinning motion of an impeller, while positive displacement pumps operate by trapping liquid into pump cavities and displacing it to pump discharge.

Centrifugal pumps are further divided into radial flow and axial flow pumps. Radial pumps move the liquid outwards from the centre of the impeller into the scrolled casing, where some kinetic energy is converted to pressure forcing the liquid out of discharge. Axial flow pumps impart energy through the lifting action of propeller-shaped vanes resulting in axial discharge.

Positive displacement pumps are divided into rotary and reciprocating types. They provide a constant volumetric flowrate at a particular speed independent of pressure and liquid characteristics, and thus are mostly used for chemical dosing.

2.5.3 Pump operating characteristics

The performance of a pump is defined by the flowrate and the total dynamic head across it. When a pump pushes water or liquid through a piping system, there is resistance to the flow from friction and inertia pressure. This resistance depends on type, size and length of pipe as well as type and number of pipe fittings.

The power consumption for a pump depends on total head and liquid flowrate. The total head, P_t, depends on the height that the liquid is raised. The performance of a centrifugal pump is defined by impeller diameter, pump speed, flowrate, head, power and fluid characteristics. A typical pump performance curve is shown in Figure 5. Pump performance with a specific impeller size is shown as a continuous curve between no-flow condition (highest head) and full flow (zero head) for a specific impeller size.

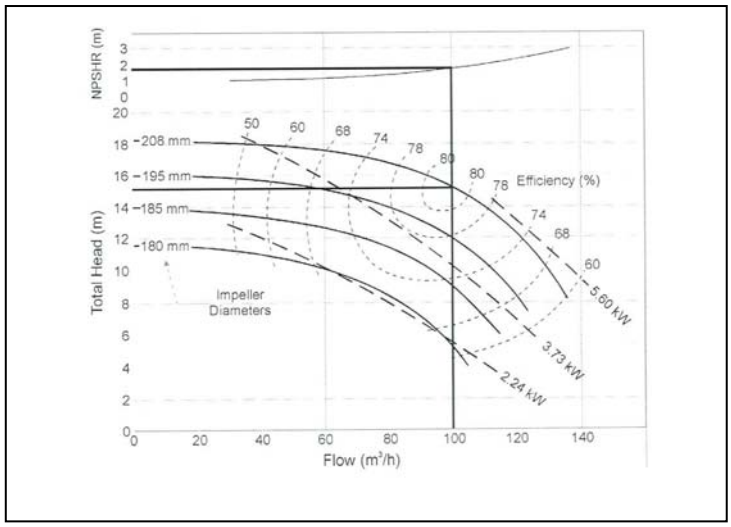

FIGURE 5: A pump performance curve

2.6 Compressed air systems

Compressed air systems are widely used in power plants to provide compressed air for system control and domestic uses. The systems consist of three main components: compressor plant (compressor, storage tanks, dryers and coolers); distribution piping network; and equipment service lines. Air compressors are grouped into positive displacements (using pistons and rotors) and dynamic displacements (using impellers or blades). They draw in air and discharge it at higher pressures, usually in storage tanks or piping systems for use in the plant.

The changes in pressure, temperature and volume of a given air mass conform to the ideal gas laws as follows:

$$\frac{P_1 V_1}{T_1} = \frac{P_2 V_2}{T_2} \tag{17}$$

where P_1, P_2 = Initial and final absolute pressures (Pa);
V_1, V_2 = Initial and final volumes (m^3);
T_1, T_2 = Initial and final temperatures (K).

The ideal gas laws can be written in terms of volumetric flowrates as:

$$\frac{P_1 Q_1}{T_1} = \frac{P_2 Q_2}{T_2} \tag{18}$$

where Q_1, Q_2 = Initial and final air flowrates (m^3/s).

However, during the actual compression processes, the ideal gas laws are not followed because the processes are non-adiabatic (heat addition or removal to the system occurs) and non-isothermal (temperature changes during the process).

2.7 Non-condensable gas extraction system

Non-condensable gas extraction systems are installed in power plants to remove gases from turbine exhaust steam, hence maintaining condenser pressure. Before gas removal, it is appreciably cooled, so as to dissolve some in water and also reduce its volume. This reduces the size/capacity of the gas extraction systems and hence their capital costs.

Steam ejectors and liquid ring vacuum pumps are the most common types of equipment used in gas extraction systems, though their selection depends on the gas content in steam. Selection of a particular system also depends on reliability, initial cost, operating costs and space requirements, and the frequency and complexity of maintenance. Steam ejectors operate by Bernoulli's principle, which relates kinetic energy and potential energy in a flow stream. The relationship is given by:

$$\frac{P}{\rho g} + \frac{v^2}{2g} + z = K \tag{19}$$

where P = Pressure in the stream (Pa);
ρ = Average density of the gases (kg/m^3);
v = Velocity of the gases (m/s);
g = Gravitational acceleration (m/s^2);
z = Elevation (m);
K = Constant.

3. METHODOLOGY

3.1 General approach

After the installation of Olkaria II plant (Appendix II), the contractor (MHI) was to run it for one year and then carry out a thorough plant inspection/maintenance before handing it over to the owner. Both these tasks (plant operation for one year and inspection/maintenance) were also supposed to be a training period for operation and maintenance staff for eventual plant operators. The operation training involved the study of PLCs (programmable logic controls), plant start-up and shut-down, problem diagnostics, designing PLCs to fit certain operating modes, etc.

In maintenance, the tasks involved understanding main equipment operations and measured parameters generated from PLCs to diagnose the plant status. The plant was divided into subsystems: turbine, condenser, cooling tower, pumps, compressed air systems, etc. and in each subsystem, operating parameters were analysed to know which part to concentrate on during maintenance. Each subsystem/equipment was opened (dismantled) according to the results of analysed measured parameters and a thorough inspection was done before correcting the problem or retrofitting.

A meeting was then held between the contractor, the owner's representative and the operation/maintenance staff where results were discussed, suggestions presented and the equipment reassembled.

3.2 Sources of data

The data used in this report were obtained from the following sources:

- Actual plant operation logs for the 10th and 30th September, 2004. The logs used included daily plant logs, turbine logs, auxiliary equipment logs, and the occurrence book (compiled together in Appendices III and IV);
- Turbine maintenance manuals for plant design parameters;
- Maintenance/Inspection report for Olkaria II plant done by MHI (Mitsubishi Heavy Industries) staff and maintenance staff for Olkaria II plant;
- Plant operation computer back-up (PLCs data) monitoring reports;
- Olkaria II plant monthly reports for availability factors, load factors, utilisation factors, etc.;
- Internet downloads for maintenance and design strategies applied in other plants in the world;
- Well discharge fluid chemistry and samples from the steam pipeline. The well discharge data used (Appendix I) is well discharge data collected during well testing after drilling; the data may have changed since then.

3.3 General assumptions and sources of error

The following general assumptions were made in the Olkaria II plant description, the maintenance strategies and the discussions of solutions:

- The non-condensable gas (NCGs) content in the steam is 0.75% by weight and mostly consists of carbon dioxide (CO_2) and hydrogen sulphide (H_2S). Traces of different gases e.g. CO, N_2, CH_4, etc. have negligible effect on well discharge chemistry and steam. Also, the NCGs content is assumed to be constant.
- Air leakage into any subsystem/equipment is assumed to be part of NCGs and does not change the properties of the gas.

- Geothermal fluid is assumed to have the properties of pure water and water vapour; the chemistry of the geothermal fluid is constant.

Sources of errors may occur from the following:

- Accuracy of measuring instruments e.g. flowrate measuring instruments are not always well calibrated and hence the results are not always conclusive.
- Though there is an automatic back-up of measured operating parameters, most of the data is from manual logs which may have human error in reading, recording and interpretation of data. The data depends on the operator's judgement.
- The chemistry of geothermal fluid and steam may have different composition since some data used was obtained during well discharge tests. The chemistry of the production wells may have changed since then, hence introducing errors and inaccuracies.
- In the analysis of deposits, the data was obtained from KenGen's laboratory and also from Mitsubishi Heavy Industries (MHI) laboratory in Japan. There may be errors during the analysis of these deposits.
- In the discussion of results, since some equipment was not opened during inspection/maintenance, it is assumed that the findings in equipment that were opened will be the same as those that were not opened, e.g. pumps.
- The values used for the reference to the environment were the mean ambient conditions. Due to variations in the local ambient conditions, mean values were used for the analysis, which may have resulted in errors.

4. OLKARIA II POWER PLANT

4.1 General plant overview

The Olkaria II power station is located in Olkaria Northeast geothermal field, which is one of seven geothermal fields in the Greater Olkaria geothermal area. The station is one of four geothermal stations currently operating in Kenya, two owned by the government and the other two owned by private developers.

The station has 2×35 MWe Mitsubishi turbines with a total installed capacity of 70 MWe, operated by the local power generating company, Kenya Electricity Generating Company Ltd. (KenGen Ltd.). The installation and commissioning of the turbines was done by Mitsubishi Heavy Industries of Japan, in the year 2002. The design and installation of the steam gathering system was done and supervised by Sinclair Knight Mertz (SKM) of New Zealand.

The geothermal reservoir is a high-temperature liquid-dominated type, with a down-hole average temperature of between 230°C and 260°C (Wambugu, 1996). The heat source of the system is magmatic intrusions located at depths of about 5 to 8 km. The fluid chemistry shows high chloride-bicarbonate waters with low pH and high gas content (0.75% in steam by weight).

Boiling starts deep in the well, and two-phase flow passes into cyclone separators tangentially, for separation at 6 bar-a. The separated steam phase passes through the steam pipeline network to the power station, while brine is injected into 4 hot re-injection wells. After a long well shut-in, the long water column is removed by blowing it into a wellhead silencer, then water passes through an open channel to a holding pod before it is pumped to 2 cold-injection wells outside the production field. The well is then connected to a steam pipeline to the station. A simplified plant layout is shown in Appendix II.

4.2 Turbine

The turbine is an impulse-reaction, single cylinder, single flow, bottom exhaust condensing turbine. The rotor is machined from a single solid forging material, supported by two journal bearings cooled/lubricated by hydraulic oil, and drives a two-pole electric generator (44 MVA) rotor through a rigid coupling. The turbine speed is 3,600 rpm.

For turbine control, a digital electro-hydraulic governor (DEH) is adopted. This consists of an electronic and hydraulic control system. The hydraulic control system has an electro-hydraulic converter, which converts electrical signals from the electric control system to control oil pressure, which then controls the turbine emergency stop and governing valves.

Saturated steam flows at a flowrate of 69.4 kg/s from single-flash cyclone separators into steam pipelines and then through a venturi-meter, steam scrubber, bucket strainers and main stop/governing valves into the steam chest. In the steam chest, point 1 (Figure 6), the steam pressure is at 4.5 bar-a, temperature at 150°C, dryness fraction about 99.6% and the non-condensable gas (NCGs) content about 0.75% of steam by weight. The steam enthalpy at turbine entry is ~2,740 kJ/kg. Steam passes into the 6-stage turbine through nozzles at high velocities and is expanded to a condenser pressure of 0.075 bar-a. In the 1st, 2nd and 3rd stages of rotating blades (impulse blades), steam pressure drops from 4.5 to 0.1 bar-a. This big drop in steam pressure is accompanied by about a 156 kJ/kg enthalpy drop and hence work is transmitted to the turbine rotor. In the subsequent stages, the 4th, 5th and 6th rows of rotating blades (reaction blades), steam pressure drops from about 0.1 bar-a to turbine exhaust pressure of 0.075 bar-a, point 2a (Figure 6). At the turbine exhaust, steam enthalpy is found to be 2,240 kJ/kg, and wetness is about 0.86. The turbine efficiency has been calculated to be 83% starting from turbine entry conditions.

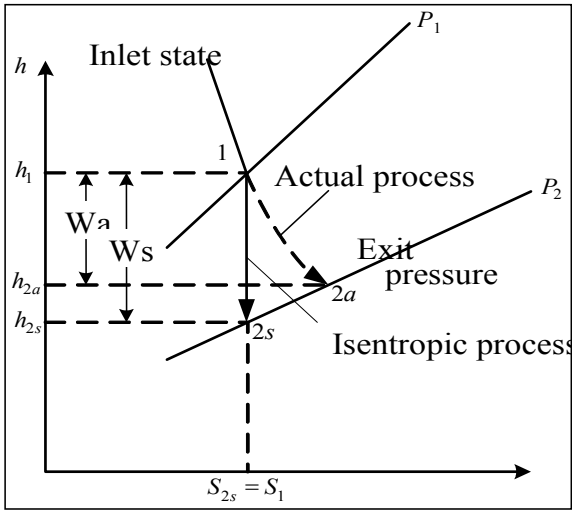

FIGURE 6: Turbine adiabatic expansion

Drain catchers are cut in the lower halves of the steam chest and turbine casing to drain the condensed steam to the main condenser. This prevents condensate carry-over to the high speed rotating blades (the 5th and 6th rows of the rotating blades) leading to blade erosion. Also, the leading edges of the 5th and 6th rows of rotating blades have stellite strips to curb blade erosion due to wet steam. Scale deposition at the nozzle throat is prevented by having a wide flow pass construction in order to minimise narrow steam passage. Stationary blades (diaphragms) are designed such that they can be removed from the turbine casings (lower and upper halves) and be cleaned in case of scale deposition.

Blade strength and turbine vibration are integral in high-speed geothermal steam turbines. Chromium-molybdenum-nickel-vanadium carbon steel is used as rotor material to resist the corrosive geothermal steam. Blades (rotating and stationary) and nozzles are made from alloyed steels high in vibration damping and durable against erosion and corrosion with the following material composition: C – 0.15%, Si – 0.5%, Mn – 0.3-0.5%, P – 0.025%, S – 0.025%, Cr – 10.5-11.0, Ni – 0.6% and Mo – 0.6% (MHI, 2000). The turbine outer casing is made of welded carbon steel plates and is a double structure composed of outer and inner casings so that it can resist erosion/corrosion. The outer casing interior is reinforced with thick plated ribs and round piped stays so that the casing is stiff enough to endure the downward load due to vacuum in the condenser.

4.3 Condenser

Olkaria II station condensers are direct-contact spray jet condensers. Each is divided into the main condenser and the gas cooler. Turbine exhaust steam (a mixture of steam and non-condensable gases), at 0.075 bar-a and 44°C, is sprayed with cold water (flowrate of 2,100 kg/s) at 24°C from the cooling tower, in the shower-deck-baffle-spray main condenser. Due to cooling, a high percentage of the steam condenses and the volume of non-condensable gases (NCGs) is considerably reduced. The NCGs then migrate to the gas cooler, where they are further sprayed with cold water flowing as jets from perforated trays (gas strainers). The gas migration is induced by the gas suction from the top of the gas cooler to the gas-extraction system. This process further reduces the volume of NCGs, hence making the size and capital cost of gas extraction equipment (the 1st, 2nd stage ejector and the liquid-ring vacuum pump) much smaller.

The mixture of cold water and the condensed exhaust steam settles at the condenser bottom and flows to the hot well pump for onward pumping to the cooling tower at a temperature of about 39°C. The pH of this mixture is about 3.5 due to dissolution of acidic gases (H_2S, CO_2, etc.) into condensate. Soda ash and biocide are added to the condensate to raise its pH to ~6.5 and prevent corrosion of piping and algae growth in the cooling tower fills.

Material selection is an integral step in condenser design due to the corrosive environment of the condensate. In Olkaria II station, the condenser shell (see Figure 7) is made from carbon steel with the interior coated with epoxy resin. This is followed by a stainless steel impingement shield (AISI 316L) about 16 mm thick, which is bonded to the carbon steel (about 20 mm) by explosion or a rolling process.

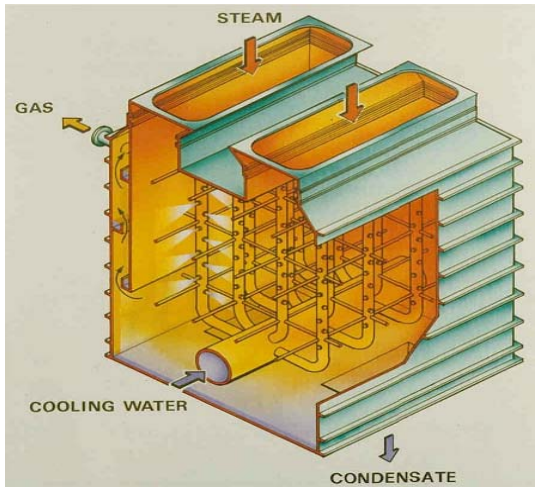

FIGURE 7: Olkaria II direct-contact condensers

4.4 Cooling tower

Olkaria II power plant cooling towers are spray and counter-flow type. They are packed with *honey-comb* plastic fills, which resist corrosion attack due to low pH (3.5) of condensate. The vertical structural supports, carrying the plastic packings/fills at the top of tower, are also made of plastic material, so as to resist corrosion attack from highly aerated condensate. The tower basin is constructed of re-inforced concrete which is then painted with epoxy resin.

At the top of the tower, a fan driven by a 70 kW motor sucks air (T=26°C, humidity=70%) from the tower bottom by induced mechanical draft. The fan is fitted with 5 plastic blades tilted at 20° which scoop air up through the fan stack. Drift eliminators are situated at the air exit, at the top of the plastic fills.

The condensate (39°C) from the condenser is pumped by hot-well pumps to the top of the cooling tower, where it is sprayed to the plastic fills. The fills are vertical sheets with rough adsorbent surfaces that wet well and allow water to fall as films that adhere to the vertical surfaces. This exposes maximum water surface area to the air without breaking it into droplets or small rivulets. The condensate flows down through the fills as air flows upwards due to fan induced suction. This counter flow cools water from about 39°C to a temperature of 24°C at the cooling tower basin, depending on ambient conditions, dissipating approximately 130 MW_t. Soda ash and biocide dosing is done in the tower basin to increase the water pH to about 6.8 and control algae growth, respectively. Water at

24°C, then flows through fibre glass plastic pipes, back to the main condenser where it is sprayed to the turbine exhaust steam in the form of jets. Air leaves the tower as a plume when it is near saturation.

The water flowrate in this recirculation cycle is about 2,100 kg/s. Excess water from the recirculation cycle is dosed with soda ash and re-injected at a pH of about 4.5-5.5, to two cold injection wells.

4.5 Non-condensable gas extraction system

Non-condensable gases (NCGs) are cooled in the gas cooler, after which the volume is appreciably decreased. The decreased gas volume, leads to reduction in size of the gas extraction systems. The gases are removed by a hybrid system consisting of a first-stage gas ejector and a liquid ring vacuum pump, which replaces the redundant second-stage gas ejector.

Motive steam, at a flowrate of 2 kg/s, is tapped from the main steam line, and passes to a convergent-divergent nozzle (first-stage steam ejector), where the high velocity of steam creates low pressure (Bernoulli's effect). The NCGs in the gas cooler, at about 30°C, are sucked by induction to this point of low pressure, where they mix with motive steam and flow to the inter-condenser. The mixture is then directly sprayed with cold water at 24°C, dissolving most gases (H_2S, CO_2, etc.) and also reducing gas volume. Also, a high percentage of the gas vapour is condensed and flows to the main condenser (see Figure 8). The cooled gases flow to the vacuum pump, where the gases are compressed and passed to the cooling tower for dispersion.

A second-stage gas ejector is redundant to the vacuum pump and only operates when the pump is out. It operates like the first-stage ejector by using tapped main steam and passing the gases through an after-condenser for more gas cooling, and finally to the cooling tower.

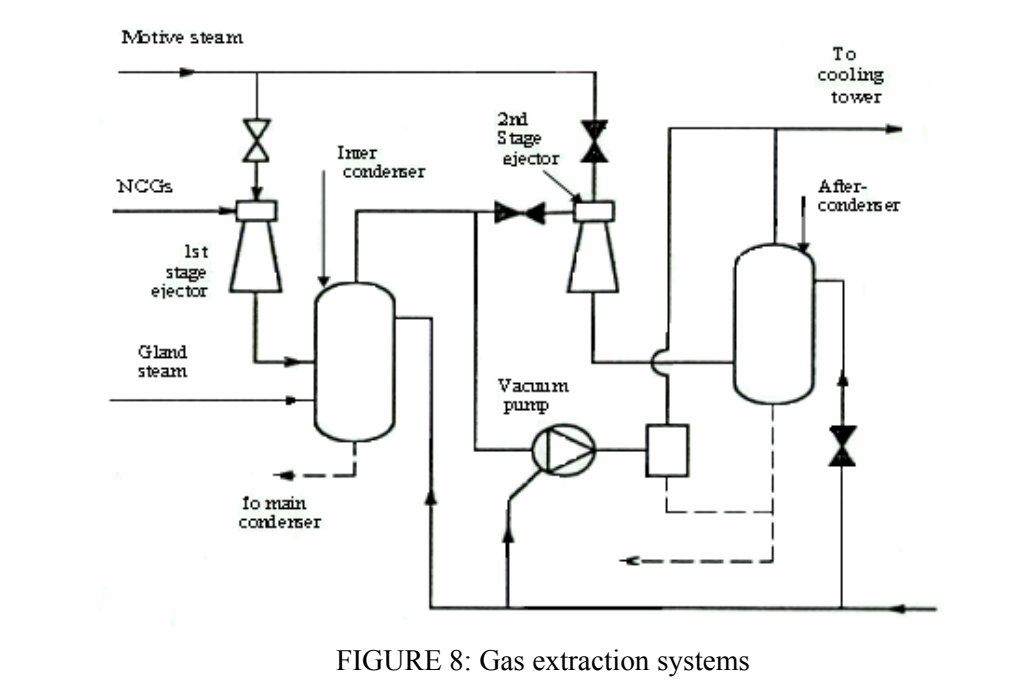

FIGURE 8: Gas extraction systems

4.6 Pumps

Olkaria II power plant is mostly equipped with centrifugal water and oil pumps, which range in size from 400 kW to the smallest 1.0 kW. Positive displacement pumps are also used for soda ash and biocide dosing into water streams for pH and algae control.

Each unit has two hot-well pumps (400 kW) and two component cooling water pumps (100 kW), which empty the condenser and supply auxiliary cooling water, respectively. The impellers are made from cast iron and they use mechanical seals, which are more durable. The hot-well pumps have a centralised vertical shaft with water-lubricated carbon bearings and pump condensate at ~1,100 kg/s at a pressure of 2 bar-a to a head of 12 m at the top of the cooling tower. The component-cooling water pumps (CCWPs) get water from the condenser suction line to supply oil coolers, generator air coolers, gas coolers, and inter- and after-condensers.

The auxiliary oil pump (AOP) and emergency oil pump supply oil to turbine bearings and control oil. The AOP supply oil during unit start-up when turbine speed is low (turbine speed < 2,700 rpm), and during unit shut-down. The emergency oil pump is a direct-current (DC) motor-driven pump used to supply oil during power black-outs.

Dosing pumps are smaller in size and mostly installed in pairs for redundancy. These pumps are equipped with ordinary stuffing boxes but mechanical seals are being considered.

5. MAINTENANCE CHALLENGES – OLKARIA II PLANT

5.1 Introduction

After a thorough analysis of the operating parameters of selected equipment, a decision was made to dismantle the equipment, inspect it and do the necessary remedial measures, which would return it to its optimal operating condition. On this annual inspection, the operating parameters were studied and found that operating/generation parameters e.g. steam flowrate, turbine steam-inlet pressure, steam chest pressure, turbine load, etc. were deteriorating. The time for annual inspection of the turbine was due, so it was decided to dismantle the main equipment of turbine 1 for maintenance.

The turbine, condenser, cooling tower, gas extraction system and pumps were dismantled and an inspection done. Since the cyclone separators' efficiency was the main suspect for the source of low steam quality, their capacities were compared with well discharge data. The pipeline was also inspected for possible heat loss due to lagging/cladding loss.

5.2 Turbine

Unit I turbine main operating parameters were analysed and found to be deteriorating as shown in Table 2. It shows that despite turbine inlet pressure, steam chest pressure, governing valves and an increasing steam flowrate, there was no corresponding increase in power output, measuring turbine efficiency at less than 83% depending on the load (Figure 9).

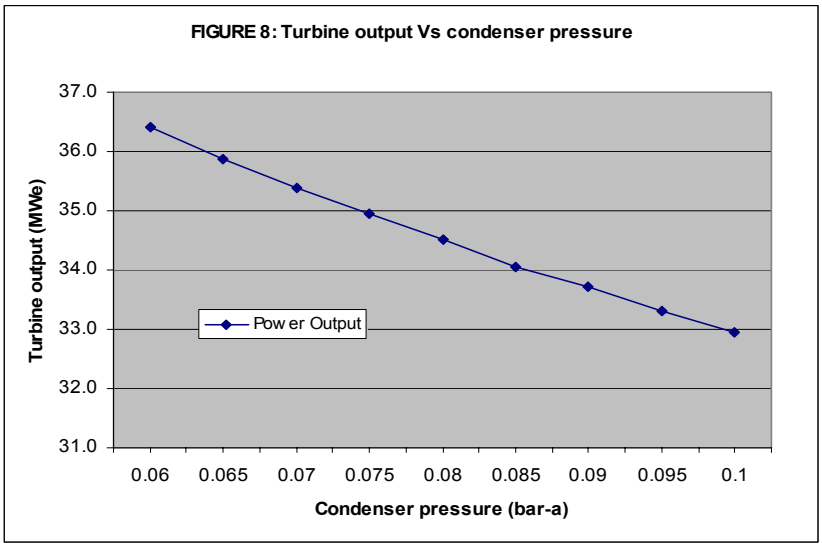

FIGURE 9: Turbine output vs. condenser pressure

TABLE 2: Unit I turbine main operating parameters before maintenance

Item	Units	Before dismantling	Design range	Remark
Power output	MWe	33.7 - 34.4	35.0	Turbine load is low
Turbine inlet pressure	bar-a	4.5	4.0	Despite inlet pressure increase, load is low
Steam chest pressure	bar-a	4.1	< 3.50	Despite blade wash, steam chest pressure is high
Steam flowrate	kg/s	72.2	69.4	Turbine uses more steam, and output is low
Control oil pressure	bar-a	6 - 8	9 ± 0.5	Control oil pressure not steady
Governor valve (GV) opening (RH)	%	> 90	65 - 75	More GV opening implies more steam required
Governor Valve (GV) opening (LH)	%	> 90	65 - 75	More GV opening implies more steam required
Utilization factor	%	< 96	> 98	Low power generation

The governor valve's opening was greater than 90% compared to a design valve of between 65% and 75%, when turbine production is 35 MWe.

After opening up the turbine upper casing, a thorough inspection was done and the following observations were made on the turbine rotor and diaphragms:

- Deposition (scale) was found around the *shroud* of the 1st row of rotating blades. The brown deposit was in 4 layers, consisting of 2 thin layers of shiny grey/white material presumed to be silica and 2 thin layers of brown/red material, presumed to be iron oxides. Maximum thickness of the scale was approximately 5 mm at the steam inlet side. The deposition was removed manually (Figure 10).

FIGURE 10: Turbine blades erosion

- The *stellite strip* outer leading edge of the 6th row of rotating blades was found to be slightly eroded. Some white rough lines moving outwards along the blades were observed and were suspected to be due to wet-exhaust steam. The white rough lines could also be observed on the 5th row of rotating blades.

- There was significant deposition around the high-pressure (HP) stage of the *1st gland seals* housing on the upper casing. One part could be due to steam leakage through the gland, depositing material on the balancing ring. The second part was due to leakage through the gland seals between the outer circumference of the gland housing and the inner mating circumference of the top casing. The deposits were hard and brittle and could be removed manually.

- The 5th and 6th stages of the *moving blade surfaces* had some pattern that looked like water marks (see Figure 10). It was thought that this was the results of blade washing, which was carried out when the turbine steam chest pressure rose to more than 3.55 bar before the inspection. This blade washing was stopped afterwards.

- Some degradation of *glands* and *inter-stage knife sealing edges* due to deposition and corrosion was noted. The rivets on the 5th and 6th stages were slightly eroded. Experience in Olkaria I plant had shown intense deposition/scaling on diaphragms making their removal difficult due to the welding action of the deposits.

- The turbine *control valves* (emergency stop and governing valves) are of the butterfly and swing-check type. These valves operate erratically with vibrations and rattling showing some wear on the main valve shafts and unstable control of the oil pressure (6-8 bar-a).

5.3 Condenser

The condenser is considered to be highly concentrated with fatal gases (H_2S, CO_2, CO, etc.) just like other enclosed areas in a geothermal environment. After opening, the condenser was evacuated for 24 hours to remove the non-condensable gases (NCGs) using a 1.5 kW centrifugal fan. This made the condenser safe for inspection while inside, though a gas detector was used to confirm the gas concentration. Also, condensate water was drained by running one hot-well pump for about 30 minutes.

During the condenser inspection, the following observations were made:

- The inner surfaces of the main condenser walls, spray pipe surfaces, and the condenser floor were all coated with about a 1 to 10 mm thick light yellow paste (Figure 11), which hardened when dry. The deposition was more pronounced at the entry ports from inter-condenser U-seal pipes.

FIGURE 11: Deposits in main condenser

- In the gas cooler, the perforations on the trays through which cold water flows to cool gas, were blocked with about 7 mm yellowish paste. The thickness of the paste increased towards the gas entry side (gas cooler bottom), making the gas cooling ineffective and leading to high condenser pressure. This made the water overflow the trays instead of going through the perforations. The approximate thickness of the yellow paste was measured from the gas cooler bottom to the top and this is shown in Table 3.

TABLE 3: Thickness of yellow paste in the gas cooler

Tray	Approximate thickness of paste (mm)
1st tray	12
2nd tray	7
3rd tray	4
4th tray	2
5th tray	0.5 & mostly clean

- The openings for the pressure switch tapings on the walls of the condenser were 50% blocked, giving erratic pressure readings for the condenser. The condenser pressure varied from 0.065-0.1 bar-a when the turbine load started to coast down.

- Slight corrosion was observed on the welds.

5.4 Cooling tower

Cooling tower inspection is considered to be risky due to its elevation and the presence of toxic gases. Safety is one aspect considered vital and involves the use of gas detectors, and other safety gear (boots, helmets, suspenders, etc.). The following observations were made during the cooling tower inspection:

- Ineffective cooling of water: the tower cooled water to 27°C instead of the design temperature of 24°C. This was noted during normal turbine operation and led to a turbine load reduction from 35 MWe to about 34.4 MWe.

- Severe corrosion was noted on all 5 fan blade attachment plates in the fan stack. These plates are made of galvanised steel with high-tensile carbon steel bolts joining them.

- The packing (plastic fills) were coated with a soft cream-yellow material (see Figure 12). Also, the spray nozzles and the water pipe supplying nozzles were getting blocked with this material approximately 3 mm thick. Samples were taken for analysis.

- Sludge was found in the cooling tower basin (< 5 mm thick) consisting of inorganic black material together with insect detritus. A sample of this material was taken for analysis.

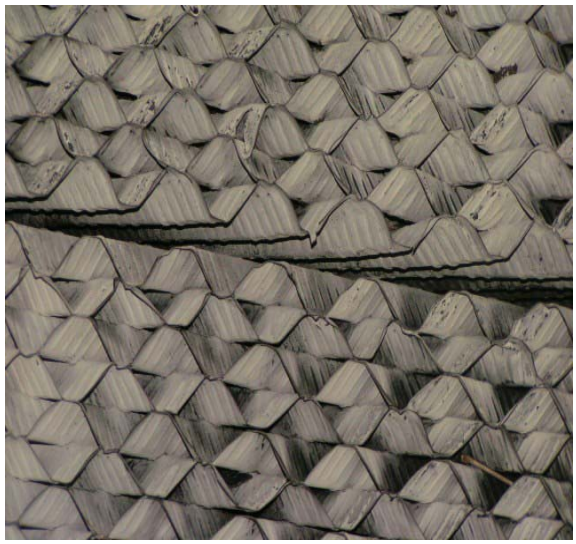

FIGURE 12: Cooling tower fills

- The fan supports (galvanized steel I-beam) showed some corrosion in the internal corners and on cut edges. Vibrations of one fan had been detected during operation.

- Slight spalling on concrete supporting the horizontal fibre glass pipe was noted.

5.5 Gas extraction system and pumps

The inspection/maintenance of the gas extraction system included the liquid ring vacuum pump, the gas ejectors, inter- and after-condensers and the NCGs piping to the cooling tower. After opening up the pump and doing internal inspection with a *boroscope*, it was found that:

- Some slight corrosion was detected on reduction gearbox teeth and a white deposit was noted on the cone surface. The erratic operation of the vacuum pump was attributed to H_2S gas attack on pump instruments and controls.

- The hot-well pump impeller housing and the suction trough were coated with about 2 mm of a light yellow material. This material softened when wet and formed a cake when dry. It was removed with a high-pressure (15 bar-a) water jet.

- Dosing pumps rubber seals of different kinds (butyl, nitril, etc.) got brittle and leakage of water was experienced. Some dosing pumps use elastic rubber in place of impeller. The rubber moves to and fro as it is pushed by oil on one side displacing some fixed amount of

solution (soda ash or biocide). The rubber gets attacked by the condensate solution and becomes brittle. Also, severe attack of biocide on seals on flanges and stainless pipe material of pipes is common.

5.6 Cyclone separators

The steam flowrate and enthalpy from a 6 bar-a separator was measured and compared with connected separator capacities. The results are shown in Table 4.

TABLE 4: Olkaria II well production and separator capacities

Well	Steam flow (kg/s)	Steam flow (T/h)	Enthalpy (kJ/kg)	Separator rating (T/h)	Remark
OW-706 & 711	17.1	61.6	1911	50	Overloaded
OW-709	21.8	78.5	1996	100	-
OW-710	6.0	21.7	1503	25	-
OW-712	7.7	27.7	1870	25	Overloaded
OW-713	5.0	18.1	1764	50	-
OW-714 &716	39.0	140.3	1894	100	Overloaded
OW-715 & 707	17.6	63.4	1348	50	Overloaded
OW-718	5.4	19.3	1087	50	-
OW-719 & 726	19.9	71.8	1285	75	-
OW-721	10.2	36.7	1572	50	-
OW-725 & 705	17.4	62.7	1360	100	-
OW-727 & 701	19.8	71.2	1761	75	-
OW-728 & 720	21.8	78.7	2165	50	Overloaded

- After two-phase separation in vertical cyclone separators, brine is put in pipelines for re-injection. Also, two-phase flow is directed into silencers during well blow-downs to remove excess water. In the separators, small stones from formation are deposited and scaling observed in concrete silencers. The weir box, V-notch and concrete water channel from silencers to the hold ponds were observed to be lined with white and black material, believed to be silica forming below a temperature of 150°C. The holding ponds were also observed to be lined with white silica at the bottom.

5.7 Other

General corrosion: General corrosion is common in all outdoor facilities and indoor electrical and electronic equipment of a geothermal power plant (Hunt, 2000). In Olkaria II plant, corrosion attack on outdoor equipment due to H_2S was noted on bus bars, clamps, conductors, multi-layered flexible copper straps, copper piping for air conditioning systems, etc. Indoor electrical equipment, especially electronic printed boards with plug-in copper connections, control, instrumentation and protection equipment had been attacked. Indoor equipment had been kept in rooms where H_2S gas was cleaned from ambient air using purafil as a H_2S scavenger and silica gel for moisture.

Main steam scrubber and steam traps: During inspection, soft black sludge at the bottom of both the main steam scrubber and steam traps was found. The sight glass for the steam traps was found to be

blurred and the water level could not be seen clearly. The isolation valve for the main steam scrubber was not sealing well due to deposition on the valve seat.

Vent silencers: Vent silencers are four in number (two in use and two redundant) and are used to vent excess steam not required by turbine. A mixture of white and black deposits, about 0.5 mm thick, and a corrosion attack were found on the valve seats and the drain pipes. The operation of the valves was erratic giving incorrect responses to steam pressure changes. An attack on the concrete foundation joint with yellowish colouration was noted. The joint was caulked.

Rupture discs: The operation pressure (4.8 bar-a) of the field was very close to the bursting pressure of disks especially during cyclicity of wells, vibrations of pipes and acoustic waves. Reverse buckling disks with a design pressure of about 90% bursting pressure were tried and have given good results.

Soda ash and hypochlorite solution tanks and piping: Before soda ash is dosed into condensate to increase pH, it is put into a solution tank for 6 hours, and then transferred to a storage tank from where dosing pumps suck the solution to the cooling tower basin and hot-well pump discharge. In the solution tank, some soda ash had settled at the tank bottom, forming a cake which blocked the tank discharge. Also, steel piping for the soda ash and hypochlorite were getting punctured and leakage was detected.

6. RESULTS AND DISCUSSION

6.1 Introduction

After turbine dismantling and maintenance, samples of two-phase brine-steam mixture, steam, scale deposits, and condensate were taken for analysis in the geochemistry laboratory. Also, well production flowrates at 6 bar-a were compared with separator design capacity to discover whether there was brine carry-over to steam pipelines, affecting steam quality.

Four samples collected from inside the turbine shroud, turbine blades, the condenser, and the cooling tower were analysed using X-ray diffraction (XRD) in Olkaria geochemistry laboratory. X-ray fluorescence was also done for element composition analysis in Japan by Mitsubishi Heavy Industries. Other samples were analysed for calcite scaling, silica scaling and corrosive components in the local laboratory.

6.2 Scale deposit

Turbine shroud: By use of X-ray fluorescence spectrometry analysis, the major elements found in the brown deposits were iron (Fe) and sulphur (S) with each element being about 5% by weight. Minor elements found were aluminium (Al) with contents of about 0.5 to 5% by weight, and other trace elements being Si, Cr, Mg, Ni, etc. being lower than 0.5% by weight. Based on these results, the estimated weight percentage of brown deposit was: Fe_2O_3 – 84%; S – 13%; SiO_2 – 1.1% and Cr_2O_3 – 0.6%.

The scale deposit in the turbine shroud is FeS_2 (pyrite/marcasite), pyrrhotite, Fe_2O_3 (magnetite) and is formed through the following reactions:

$$Fe + 2HS^-_{(aq)} + H^+_{(aq)} = FeS_{2\,(s)}\ (pyrite) + 2H_{2\,(g)}$$

$$Fe + H^+_{(aq)} + HS^-_{(aq)} = FeS_{(s)}\ (pyrrhotite) + H_{2\,(g)}$$

$$3Fe + 4H_2O = Fe_3O_{4(s)}\ (magnetite) + 4H_{2(g)}$$

Turbine blades: The brown and white deposits on the turbine blades were analysed using X-ray diffractometry, and the contents were found to be: Alfa Fe_2O_3 (hematite-brown), Fe_2O_3 (magnetite-black), Fe_2S_2 (pyrite-yellow), and Fe_3O_4 (marcasite-grey-yellow).

Discussion: The scale deposit is formed from the reaction of iron-rich impurities in the steam to hydrogen sulphide gas (H_2S). During steam condensation, H_2S gas dissolves into steam condensate to form a solution where it dissociates and becomes reactive, forming pyrite and pyrrhotite after reaction with iron. Magnetite is formed by dissolution and dissociation of CO_2 gas. The source of iron may be from carry-over into the steam pipes during two-phase separation in cyclone separators or from transmission pipelines. It is reported that pyrite is a common hydrothermal mineral in Olkaria Northeast field where it occurs at deeper levels, especially in well OW-716 (Agonga, 1992).

Scale is thought to have deposited at turbine nozzles constricting the steam path, leading to turbine inlet and steam chest pressure increases from 4.0 to 4.5 bar-a and from 3.6 bar-a to more than 4.0 bar-a, respectively. This is thought to be the main cause of low turbine productivity (slightly above 34 MWe). After cleaning the shroud manually by removing the deposit, the turbine load, steam inlet pressure, and steam chest pressure improved.

The erosion on the stellite strip could be attributed to excess steam wetness (wetness fraction > 0.14) at the turbine exhaust, and water droplets during turbine blade wash, which are thrown radially outwards by the centrifugal force of turbine high-speed blades. The high moisture content causes blade erosion as a result of the impingement of water droplets on the blades, surface washing, and the so-called *wire drawing* caused by high-velocity water/moisture leaking through narrow passages (El-Wakil, 1984). Since the lower turbine casing is designed to have drain holes (to drain condensate to condenser), it was found that the holes were clogged with iron compound deposits found at the shroud of the 1st stage moving blades.

Condenser and cooling tower deposits: After testing and analysing the deposits found in the condenser and cooling tower fills, it was found that sulphur (orthorhombic sulphur) is the dominant compound. Sulphur mixes with insoluble soda ash to settle at the bottom of the cooling tower basin as a mud which can be removed by manual cleaning.

Discussion: In direct-contact condensers, a big portion of H_2S gas dissolves in the cooling water due to high gas solubility. Also, the cooling water from the cooling tower is saturated with oxygen gas, which is a strong oxidizing agent for H_2S gas. Depending on the pH of the cooling water, sulphur is deposited in various forms according to the following reactions:

$$H_2S_{(gas)} + 2O_{2\ (gas)} = 2H^+_{(aq)} + SO_4^{2-}{}_{(aq)}$$

$$SO_4^{2-}{}_{(aq)} = S^{2-}_{(aq)} + 2O_{2\ (gas)}$$

These reactions take place in the presence of water, and sulphur is deposited in the condenser and cooling tower. Sodium was detected in the sludge indicating that the dosing chemical, which is mainly composed of Na_2CO_3 and $NaHCO_3$ (soda ash) does contribute to the sludge deposition. Sulphur is also formed by partial oxidation of H_2S as per reaction:

$$2H_2S_{(aq)} + O_{2\ (g)} = 2S_{(s)} + 2H_2O$$

This reaction is highly kinetically favoured and further oxidation of sulphur to sulphate is accelerated by bacterial content (algae), and high pH of water. Constant inspection (biannually) is required for cleaning the condenser and the cooling tower to prevent the paste from affecting turbine loading.

Steam scrubber, steam traps and vent station: The analysis of samples collected from the steam scrubber gave the following composition by weight: iron (36.67%), silica (0.91%), calcium (0.04%) and traces of sulphur. In the vent station, the dominant compound was silica (37.70%) and iron compounds (6.09%).

Discussion: The compounds found in these facilities are formed from the reaction of H_2S gas with iron rich impurities in moisture entrained in steam. Silica forms when steam condensate with carry-over from the separator cools to a temperature below silica saturation temperature, at about 150°C. The black sludge drained from the steam scrubber and the steam traps is an iron-rich compound. To prevent the black sludge depositing and hardening, thereby affecting the operation of the equipment, it is always necessary to drain them after variable intervals. Removal of small pieces of stones from the formation can be done during the annual inspection of the whole plant.

6.3 Corrosion

Corrosion in geothermal environments is attributed to corrosive species which are in mixture with steam, brine carry-over, and a cooling water circulation system: oxygen gas; hydrogen ions; carbon dioxide species (dissolved CO_2 gas, bicarbonate ion, and carbonate ion); hydrogen sulphide species (H_2S gas, bisulphide ion, sulphide ion); chloride ion and ammonia species (ammonia and ammonium ion).

Oxygen: Oxygen is extremely corrosive to carbon and low-alloy steels which are the main constituents of geothermal installations. Above concentrations of 30 ppb, it causes a fourfold increase in the carbon steel corrosion rate; concentrations above 50 ppb cause serious pitting (MHI, 2000). Oxygen attack is even more severe on austenitic stainless steels in the presence of chloride ions, moisture and high temperature when it causes chloride–stress corrosion cracking (chloride SCC). The attack can be minimized by painting to prevent chloride ions and moisture ingress.

Hydrogen ion (pH): Hydrogen ion is a major component of geothermal fluid and steam condensate due to the dissolution of acidic gases and fluid-rock interactions deep in a reservoir. It's responsible for the primary cathodic reaction of steel in a air-free brine as well as acid attacks on cements. In low pH environments, it causes a breakdown of passivity of stainless steels and promotes sulphide stress cracking of high-strength low-alloy steels and other alloys coupled to steel.

Carbon dioxide species: CO_2 gas dissolves in condensate, lowering its pH and increasing carbon and high-strength low-alloy steel corrosion attacks. It exacerbates stainless stress cracking in low-temperature geothermal wells.

Hydrogen sulphide species: Hydrogen sulphide species are highly corrosive to alloys containing copper and nickel, such as in conductors, air conditioning systems, electronic devices, etc. They also promote sulphide stress cracking (SSC) and accelerate attacks on high-strength low-alloy steels (HSLA). The attack noted on the cooling tower fan plate is attributed to hydrogen sulphide species. Smearing the plate with thick oil was tried but it gets washed away after awhile.

Chloride species promote the localised corrosion of carbon, HSLA, and stainless steel as well as other alloys. Pitting corrosion is solely attributed to chloride species though steel passivates at high temperature in pH 5 and at 6,070 ppm chloride concentrations. Ammonia species are not common in geothermal environments but cause SCC (MHI, 2000).

6.4 Cyclone separators

The cyclone separators are vertical cylinders and two-phase fluid from the well enters tangentially almost half way up the separator. Wells have individual separators while others are shared depending on well flowrates and locality (Table 4). When the separator capacity is lower or equal to the steam flowrate from the well(s), then the separator becomes overloaded or very near to being overloaded. During the separation process in overloaded separators, liquid is entrained in steam leading to scaling and/or the corrosion of piping and turbine blades. Though there are steam traps and a steam scrubber just outside the turbine inlet for condensate removal, the wet steam carries dissolved solids like silica leading to turbine scaling and corrosion on nozzles and blades. At higher well flowrates, steam quality drops significantly due to low enthalpy of well fluids: for an enthalpy of 1,800 kJ/kg and a 50 tons/h separator, the steam quality dropped from 99.98% to 99.90% when the enthalpy was lowered to 1,400 kJ/kg. This calls for the up-rating of all separators with capacities lower or near to the well flowrates.

After operating vertical separators for many years, experience has shown that they are less efficient compared to horizontal separators (Svartsengi power station). It is recommended that future construction of separators in Olkaria power station be of the horizontal variety.

7. CONCLUSIONS AND SUGGESTIONS

From the results and discussion, it can be concluded that:

- The deposits on the turbine shroud and blades are mainly the product of iron and hydrogen sulphide/carbon dioxide gases reacting to water to form pyrite (FeS_2), magnetite (Fe_3O_4) and iron oxides. The iron might be coming from deep in the reservoir or from mild steel pipelines, finding its way into steam pipelines via brine carry-over due to over-loaded separators.

- The erosion of the stellite strip and 6^{th} stage blade surfaces is attributed to excess wetness of exhaust steam and also water droplets from blade washing.

- Sulphur is the dominant compound deposited in the condenser and cooling tower giving a paste of light yellow colour. It is believed to be formed from partial oxidation of hydrogen sulphide gas.

- The attack on electronic gadgets and the blackening of electrical conductors is due to hydrogen sulphide (H_2S) gas. Other acidic gases, e.g. CO_2, SO_2, etc. also contribute to corrosion attacks on conductors and other metallic materials in the plant surroundings, though to a lesser extent.

- The low efficiency of the vertical cyclone separators is attributed to brine carry-over into steam pipelines, which causes deposition in the turbine and other facilities due to mineral dissolution. The brine in the steam is mainly caused by carry-over in the cyclone separators as no steam condensation due to heat loss was suspected.

Following are suggestions for the operation of the plant:

- Use of high-alloy chromium steels should be used for endangered parts or shielding exposed areas with similar material to curb erosion/corrosion on the turbines. It has been found that 12%-13% chromium steel does not suffer erosion corrosion at all (Moore and Sieverding, 1976).

- The separators which are overloaded should be up-rated so that the separator capacity is higher than well(s) flowrates, to give high steam quality after separation. Also, horizontal separators, which give high separation efficiency, should be tried (as experienced in Svartsengi power plant, Iceland).

- Blade washing should be stopped temporarily, blade erosion monitored at the next inspection, and steam scrubbing started. Also, the condensate drain holes on the lower turbine casing need to be unblocked during each annual turbine inspection.

- The pH of re-circulating water from the cooling tower to the condenser needs to be maintained at between 6.5 and 7.5 to inhibit the deposition of sulphur. During current plant operation, the pH is erratic due to inconsistency in soda ash dosing or incorrect readings from instruments.

- All the sensitive electronic devices should be kept indoors where air is free from hydrogen sulphide (H_2S) and other acidic gases. Coupons made from copper and aluminium need to be placed at strategic points to monitor H_2S attacks in the plant as is done in the Krafla power station, Iceland. Outdoor electronic devices needs to be kept in locked pressurised cabinets and exposed parts smeared with *vaseline* or *epoxy*.

- Corrosion inhibitors in re-circulating water, such as chromates and scale inhibitors e.g. *polyelectrolytes* (which keep deposit particles suspended in water and precipitate in the cooling tower basins, where they can be removed as mud) should be used.

- Steam scrubbing should be implemented to clean steam. In this operation, condensate is pumped into steam pipelines on the upstream of a steam scrubber. The condensate is then removed from the scrubber by draining off. Also, the conductivity of steam needs to be closely watched to monitor the concentration of solutes, related to steam wetness.

- Improvement can be made in the condenser by installing a pump and some piping to clean the gas cooler trays with high-pressure water (> 30 bar-a) during the machine operation, as is done in Krafla power station.

ACKNOWLEDGEMENTS

I wish to express my sincere gratitude to the Government of Iceland, The United Nations University – Geothermal Training Programme (UNU-GTP) and my employer, Kenya Electricity Generating Company Ltd. (KenGen) for giving me the opportunity to participate in the 28th session of the UNU-GTP. My gratitude goes to Dr. Ingvar B. Fridleifsson, the Director of UNU-GTP, Mr Lúdvík S. Georgsson, the Deputy Director, UNU-GTP and Mrs. Gudrún Bjarnadóttir and Ms. Thórhildur Ísberg, the Administrative Assistants, UNU-GTP, for their guidance, assistance and care throughout the course. I wish to extend my gratitude to the staff of Iceland Geosurvey (ISOR) and Orkustofnun for sharing their time and resources with us and for their comprehensive lectures and presentations during the course. Also, my gratitude is extended to Reykjavík Energy, Hitaveita Sudurnesja, and the University of Iceland among others for their unrelenting support.

My special thanks go to my supervisor, Engineer Geir Thórólfsson and all the staff of Svartsengi and Krafla power stations for their dedicated support and guidance during project preparation, research and writing, which made it possible for me to complete this report. To all UNU Fellows, I am grateful for your company, support and the sharing we had during the six months of training.

Last but not least, I am grateful to my dear wife, Lydia and son Dennis, for their endurance, emotional support, prayers, and encouragement throughout the course and my stay in Iceland. Be blessed.

REFERENCES

Agonga, O., 1992: *Geothermal geology: stratigraphy and hydrothermal alteration of well OW–716, Olkaria geothermal area, Kenya.* UNU-GTP, report 10, Iceland, 44 pp.

Bore K., B., 2005: *Exergy analysis of Olkaria I power plant, Kenya*. Report 5 in: *Geothermal training in Iceland 2005.* UNU-GTP, Iceland, 2005, 1-37.

Clarke, M.C.G., Woodhall, D.G., Allen, D., and Darling, G., 1990: *Geological volcanology and hydrological control on the occurrence of geothermal activity in the area surrounding Lake Naivasha, Kenya with coloured 1:100,000 geological maps.* Ministry of Energy, Nairobi, 138 pp.

Dipippo, R., 2005: *Geothermal power plants: Principles, Applications and case studies.* Elsevier Ltd. Kidlington, UK, 450 pp

El-Wakil, M.M., 1984: *Power plant technology.* McGraw-Hill Company, USA, 861 pp.

Gunnarsson, I., Arnórsson, S., and Jakobsson, S., 2005: *Precipitation of poorly crystalline antigorite under hydrothermal conditions*. University of Iceland, Institute of Earth Sciences, 15 pp.

Hart, W., 1979: *Final report on direct contact condenser tests carried out on the Ohaaki/Broadlands pilot plant*, New Zealand Electricity, Wellington, 10 pp.

Hunt, I., 2000: Electrical planning and design for geothermal power project. *Proceedings of the World Geothermal Congress 2000, Kyoto-Tohoku, Japan*, 3183-3188.

Lagat, J.K., 2004: *Geology, hydrothermal alteration and fluid inclusion studies of the Olkaria Domes geothermal field, Kenya.* University of Iceland, MSc. thesis, UNU-GTP, Iceland, report 2, 71 pp.

Lichti, K.A., and Braithwaite, W.R., 1980: Surface corrosion of metals in geothermal fluids at Broadlands, New Zealand. *Geothermal scaling and corrosion, ASTM STP, 717*, 97-105.

Opondo, K.M., 2002: Corrosion tests in cooling circuit water at Olkaria I plant and scale predictions for Olkaria and Reykjanes fluids. Report 10 in: *Geothermal training in Iceland in 2002. UNU-GTP, Iceland,* 147-186.

Ofwona, C., 2002: *A reservoir study of Olkaria East geothermal system, Kenya*. University of Iceland, MSc. thesis, UNU-GTP, Iceland, report 1, 74 pp.

MHI, 2000: *Air quality impact assessment: Olkaria II geothermal power plant project hydrogen sulphide dispersion study using revised emissions*. Holmes Air Sciences, Japan, 25 pp.

Moore, M.J. and Sieverding, C.H., 1976: *Two-phase steam flow in turbines and separators*, Hemisphere Publishing Corporation, USA, 399 pp.

Wambugu, J.M., 1996: Assessment of Olkaria northeast geothermal reservoir, Kenya, based on well discharge chemistry. Report 20 in: *Geothermal training in Iceland in 1996.* UNU-GTP, Iceland, 481-509.

World Energy Council, 2004: *Survey of energy resources*. (20th edition). Elsevier Ltd., UK, 456 pp.

APPENDIX I: Chemical composition of well discharges for Olkaria Northeast field, water phase concentration in ppm, (Wambugu, 1996)

Well No.	WHP (bar-g)	GSP (bar-g)	Enth. (kJ/kg)	pH	B	SiO_2	Na^+	K^+	Mg^{2+}	Ca^{2+}	F^-	Cl^-	SO_4^{2-}	CO_2	H_2S
OW-701	11.7	4.5	1153	9.4	3.2	686	542	125	0.2	0.7	45	714	18	128	5.3
OW-703	8.39	4.94	1257	9.2	1.2	886	710	176	0.1	0.2	83	884	24	217	1.42
OW-705	4.07	2.97	1468	9.28	-	768	534	68	0	0	64	463	17	251	11.9
OW-706	6.41	4.83	1851	9.28	3	822	510	107	0.13	0.04	68	642	32	194	3.1
OW-707	7.24	2.9	1752	9.16	4	875	520	97	0	0	53	621	140	150	8
OW-709	6.3	1.88	1954	9.45	5.5	873	830	213	0	0	164	789	53	290	4.1
OW-710	8.28	2.76	1082	8.73	1.7	396	448	98	0	0	40	517	22	198	1.4
OW-711	5.77	2.76	1233	9.14	1.3	706	554	120	0	0	70	569	29	245	6.46
OW-712	4.48	2.62	2036	9.82	4.4	796	710	82	0	0	46	590	63	155	6.8
OW-713	2.76	2.07	1696	9.14	1.5	741	517	78	0	0	30	574	26	224	7.14
OW-714	17.93	2.76	1454	9.58	3.8	850	620	118	0	0	54	642	33	186	2.7
OW-716	3.59	2.76	2645	6.77	6.9	438	535	110	0.33	0.2	28	797	90	58	0.44
OW-718	8.28	2.76	956	9.44	4.3	694	500	80	0	0	51	474	41	152	3.1
OW-719	6.55	2.9	1167	9.5	3.3	753	540	87	0.3	0.2	46	507	39	198	6
OW-721	10.34	2.07	1706	9.61	3	845	650	77	0	0	62	468	71	193	10
OW-725	6.6	-	1380	9.85	5	677	700	88	0	0	58	588	34	247	27
OW-726	6.76	2.97	1602	8.9	5	785	570	88	0	0	37	675	61	167	7.8
OW-727	5.52	3.03	1720	8.54	4.2	818	500	67	0	0	37	576	77	147	5.1

APPENDIX II: Olkaria II plant layout

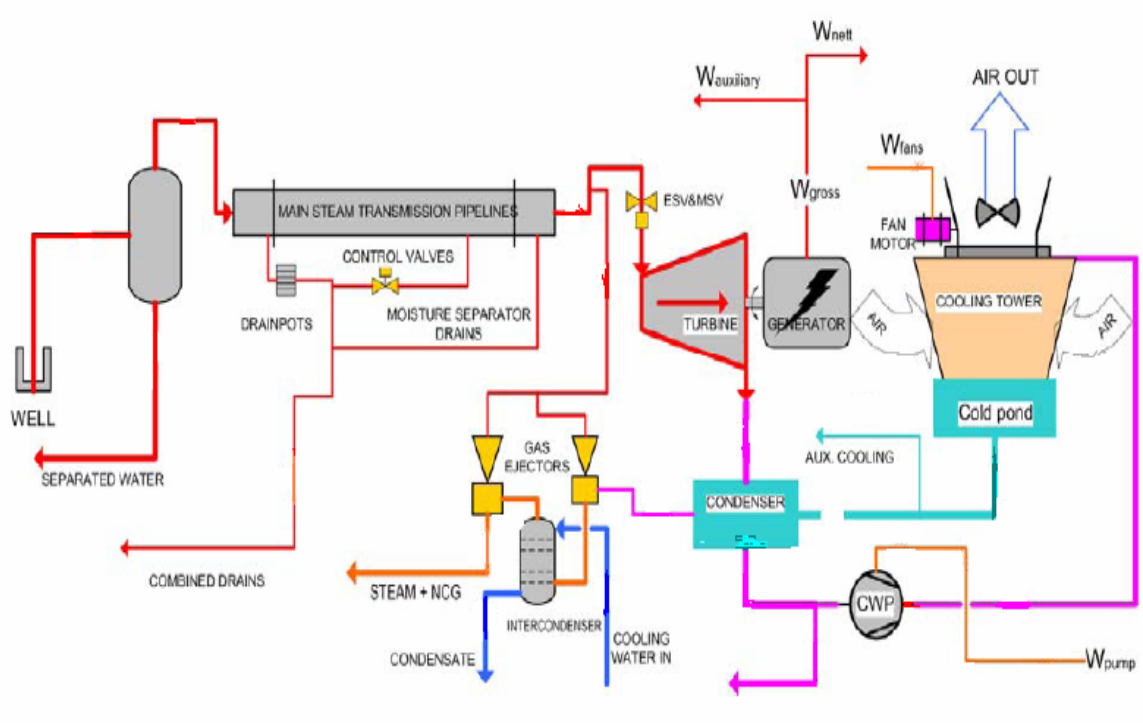

APPENDIX III: Plant/turbine logs before inspection

Item Description	Units	08:00	10:00	12:00	14:00	16:00	18:00	20:00	22:00	24:00:00	02:00	04:00	06:00
Unit load	MWe	33.8	34.2	33.9	34.3	34.1	34.4	33.9	34.1	33.7	33.8	33.8	34.1
Turbine speed	rpm	2987	3004	3005	3007	2998	3000	2999	2997	3011	3005	2989	2997
Vent station steam pressure	bar-a	4.75	4.75	4.76	4.77	4.77	4.77	4.76	4.76	4.76	4.77	4.76	4.77
In-line steam PCV opening	%	99.7	99.1	96.5	93.8	98.9	98.6	99.9	99.8	99.9	100.2	100.2	100.2
Lead vent station PCV opening	%	12.3	10.3	5.2	0	9.5	0	12.4	12.1	13.5	19.2	17.3	19.7
Main steam flow rate	T/H	259.7	260.7	258	259.4	256.6	258.5	261.7	259.7	258.9	259.7	257.6	259.8
Main steam temp. (scrubber inlet)	°C	153.7	153.6	153.5	153.5	153.6	153.6	153.6	153.6	153.6	153.6	153.6	153.5
Main steam press. (scrubber inlet)	bar	4.6	4.6	4.6	4.5	4.6	4.6	4.6	4.5	4.6	4.6	4.6	4.6
Steam scrubber level	mm	647	685	712	723	750	770	786	811	620	628	649	664
Steam scrubber level control v/v opening	%	0.7	0.8	0.8	0.8	0.8	0.8	0.8	0.7	0.8	0.8	0.7	0.8
Main steam temp. (turbine inlet; LH)	°C	151.1	150.9	150.8	150.8	150.9	151	151	151	151	151	151	151
Main steam temp. (turbine inlet; RH)	°C	153.5	153.3	153.8	153.3	153.4	153.4	153.4	153.4	153.5	153.5	153.4	153.4
Main steam press. (turbine inlet; LH)	bar	4.5	4.4	4.4	4.5	4.5	4.5	4.5	4.5	4.5	4.4	4.5	4.5
Main steam press. (turbine inlet; RH)	bar	4.5	4.5	4.4	4.5	4.4	4.5	4.4	4.4	4.5	4.4	4.4	4.4
Main steam coductivity	µMHO	45	50	45	60	45	44.6	44.8	44.8	44.8	45.2	55	45.4
Condenser vacuum pressure	bar-a	0.088	0.09	0.09	0.091	0.094	0.09	0.089	0.089	0.088	0.085	0.088	0.084
Auxiliary steam header pressure	bar-g	4.6	4.6	4.6	4.6	4.6	4.6	4.6	4.6	4.6	4.6	4.6	4.6
Auxiliary steam header temp.	°C	154.2	154	154	154	154.2	154.1	154.2	154.2	154.3	154.2	154.3	154.3
Auxiliary steam flow	T/H	14.8	14.7	14.7	14.7	14.7	14.7	14.7	14.7	14.7	14.7	14.7	14.7
Ejector steam supply header pressure	bar	4.5	4.5	4.5	4.5	4.5	4.5	4.5	4.5	4.5	4.5	4.5	4.5
Turbine gland steam pressure	bar	0.23	0.22	0.22	0.22	0.23	0.23	0.22	0.22	0.23	0.22	0.22	0.23
Turbine gland steam PCV opening	%	35.7	35.6	35.6	35.6	35.5	35.6	35.7	35.6	35.6	35.6	35.7	35.7
Lube oil pressure at cooler outlet	bar	1.73	1.75	1.75	1.75	1.74	1.73	1.74	1.74	1.74	1.74	1.74	1.75
Main oil tank level	mm	-37.3	-38.8	-37.7	-37.6	-37.3	-38.6	-38.9	-37.9	-39.3	-39.4	-39.8	-41.1
Main oil tank oil temperature	°C	60.8	61.5	61.8	62.1	62.3	61.8	61.5	61.4	61.1	61.2	61.1	60.8
Oil cooler outlet oil temperature	°C	44.2	44.8	45.2	45.2	45.5	44.9	44.6	44.6	44.3	44.3	44.2	43.9
Control oil pressure	bar	7	6.5	8	6.5	6.5	7	6.5	8	7.5	8	7.5	7.5
E/H converter (R/H) pressure	bar	2.92	4	4	2.32	4	4	0.66	1.11	1.87	4	0.23	0.18
E/H converter (L/H) pressure	bar	3.9	1.86	2.69	3.21	3.06	4	1.63	3.76	3.2	1.53	1.73	1.64
No. 1 bearing metal temperature	°C	69.4	69.8	70.1	70.3	70.4	69.8	69.7	69.7	69.5	69.4	69.5	69.2
Thrust bearing metal temp. (Gov. side)	°C	60	60.5	60.8	60.9	61	60.4	60.3	60.3	60.1	60.1	60.1	59.8
Thrust bearing metal temp. (Gen. side)	°C	51.5	52.1	52.4	52.6	52.7	52.2	51.9	52	51.8	51.7	51.8	51.4
No. 2 bearing metal temperature	°C	66.1	66.6	66.8	67	67.1	66.6	66.4	66.4	66.3	66.3	66.3	66.1
No. 3 bearing metal temperature	°C	68	68.6	68.6	68.8	69.1	68.4	68.3	68.4	68.3	68.2	68.3	68
No. 4 bearing metal temperature	°C	63.6	64	64.4	64.5	64.7	64.2	63.9	64	63.8	63.8	63.8	63.5
No. 1 bearing vibration (X/Y)	µm	12:13	12:13	12:13	12:13	12:13	12:13	12:13	12:13	12:13	12:13	12:13	12:13
No. 2 bearing vibration (X/Y)	µm	15:15	14:16	15:15	15:15	15:16	14:16	15:16	14:15	15:16	14:15	14:16	15:16
No. 3 bearing vibration (X/Y)	µm	21:17	22:17	22:17	22:18	22:18	23:18	23:19	22:18	23:18	22:18	23:19	22:18
No. 4 bearing vibration (X/Y)	µm	19:33	19:33	19:35	19:32	19:13	20:33	20:33	20:33	19:34	20:34	20:34	20:34
Turbine rotor position	mm	-0.14	-0.14	-0.14	-0.14	-0.14	-0.14	-0.14	-0.14	-0.14	-0.14	-0.14	-0.14
Turbine differential expansion	mm	1.53	1.52	1.52	1.5	1.48	1.49	1.49	1.49	1.52	1.52	1.52	1.53
Governing valve (LH) opening	%	96	99.7	98	98.8	99.6	97.8	99.6	97.8	99.8	99.7	98.9	98.7
Governing valve (RH) opening	%	99.7	99.7	97.6	99.4	99.6	99.7	99.5	97.8	97.5	99.7	99.5	98.4
Turbine steam chest pressure	bar-a	4	3.95	4	4.05	3.95	4	4	3.95	4.1	4	4	3.98
Turbine exhaust steam pressure	bar-a	0.089	0.09	0.091	0.092	0.094	0.09	0.089	0.089	0.087	0.086	0.088	0.085
Turbine exhaust steam temperature	°C	44.7	45.3	45.6	45.9	46	45.2	45.1	45	44.6	44.3	44.5	44
Condenser level	mm	1404	1246	1240	1403	1478	1434	1335	1308	1390	1354	1351	1404
Hot well water temperature	°C	41.5	41.9	42.1	42.4	42.6	41.7	41.6	41.6	41.4	41	41.3	40.8
Circulating water FV (gas cooler)	%	35.4	35.3	35.3	35.3	35.3	35.3	35.3	35.3	35.3	35.4	35.3	35.3
Circulating water FV (condenser)	%	62.8	62.8	62.7	62.7	62.8	62.8	62.7	62.8	62.8	62.8	62.7	62.8
Hot well pump No. 1 vibration (X/Y)	mm/s	2.3:3.5	2.3:3.4	2.1:4.0	2.1:3.6	2.0:3.5	2.2:3.4	2.4:3.6	2.3:4.5	2.2:3.9	2.2:3.7	2.2:4.0	2.5:3.8
Hotwell pump 1 stator winding temp.	°C	127.3	128.3	133.1	134	133.9	131	130.4	129.7	127.1	126.4	126.1	125.6
Hotwell pump 1 motor inner bearing metal temp.	°C	51.5	52.6	57.3	58.2	57.2	54.6	54.3	53.8	50.7	49.8	50.3	48.8
Hotwell pump 1 motor outer bearing metal temp.	°C	79.5	80.5	85.2	86.2	85.6	83.1	82.3	82	79	78.3	78.7	77.5
Hotwell pump 1 recirculation v/v opening	%	0.4	0.4	0.4	0.4	0.4	0.4	0.4	0.4	0.4	0.4	0.4	0.4
Hotwell pump 1 discharge v/v opening	%	63.3	58.8	57.6	57.8	59.5	61.2	61.5	58.2	62.5	58.5	58.1	60.3
Hot well pump No. 2 vibration (X/Y)	mm/s	1.8:2.0	1.8:1.7	1.5:1.6	1.5:1.5	1.6:1.7	1.6:1.7	1.8:1.7	1.9:1.6	1.8:1.6	1.5:1.7	1.6:2.0	1.9:2.2
Hotwell pump 2 stator winding temp.	°C	125	125.7	130.1	132.7	130.3	129.2	127.7	127.7	126.4	124.5	124.5	123.5
Hotwell pump 2 motor inner bearing metal temp.	°C	48.6	49.7	54.7	55.4	53.7	51.7	50.9	50.4	50.1	48.2	47.7	46.2
Hotwell pump 2 motor outer bearing metal temp.	°C	69.2	70.5	75.9	76.8	75.4	73.2	72.2	71.8	71.1	69.1	69	67.5
Hotwell pump 2 recirculation v/v opening	%	0.8	0.8	0.9	0.9	0.8	0.8	0.8	0.8	0.8	0.8	0.8	0.8
Hotwell pump 2 discharge v/v opening	%	64.5	59	62.1	59.3	61.1	60.9	61.5	62.2	61.5	62.3	62.2	61.6
Hotwell discharge header pressure	bar	1.8	1.7	1.7	1.7	1.7	1.7	1.7	1.7	1.7	1.7	1.7	1.7
Hotwell discharge header temperature	°C	41.6	42.2	42.8	43.1	43.2	42.3	42.1	42	41.6	41.2	41.5	40.9
C/T to condenser water flow rate	T/H	7461	6894	7377	7438	7411	7429	7558	7188	7600	7282	7161	6729
C/T basin upstream water level	mm	777.3	758.7	717.3	714.6	759.5	768	730.2	711.3	766.8	760.2	748	742.1
C/T basin downstream water level	mm	727.4	710.5	665.5	661.7	707	715.8	676.8	659	713.3	705.9	694.2	685.5
C/T fan 1 motor winding temp.	°C	74.5	76.7	80.7	81.5	78.8	77.2	76.5	76.3	73.4	74.5	74.9	73.7
C/T fan 2 motor winding temp.	°C	71.6	73	76.7	78.5	77.6	74.5	73.4	73.1	70	70.3	70.7	69.6
C/T fan 3 motor winding temp.	°C	71.4	73.5	77.8	79.2	77.5	74.3	73.4	73.1	69.5	70.4	70.4	69.4
C/T fan 4 motor winding temp.	°C	71.9	73.6	77.2	79.2	78.4	75.2	74.5	74.2	70.7	71.1	71.4	70.3
C/T fan 1 gearbox vibration	mm/s	11	11.9	13.9	10	8.6	8.9	12	9.5	11.3	12.9	8	13.2
C/T fan 2 gearbox vibration	mm/s	14.4	13.4	12.3	10.8	12.2	11	11.7	10.7	13.8	12.6	12	14.2
C/T fan 3 gearbox vibration	mm/s	11.4	13.8	11.5	11.7	9.2	11.9	11.2	13.6	11	14.5	9.4	9.8
C/T fan 4 gearbox vibration	mm/s	14.5	12.3	10.7	11	10.8	13.7	13.7	10.6	15.2	14.5	13.4	13.1
Cond. Reijection pump disch. Header pressure	bara	12.7	12.8	12.7	1.8	1.8	12.7	12.7	12.8	1.8	12.8	12.8	12.8
Cond. Reinjection pump discharge flowrate	T/H	67.9	69.2	68.4			68	68.4	68.4		68.7	68.5	68.4
Cond. Reinjection pump discharge pH	pH	7.3	7.1	7	7	6.3	7	7.2	7	6.7	7.1	7	6.9
Inter-condenser inlet gas header temp.	°C	30.7	31.2	33.6	33.7	33.8	32.9	29.7	31	30.6	30.5	30.6	30.2
Inter-condenser inlet gas header press.	mbar	121.5	126.3	141.6	141.7	141.8	137.1	145.2	123	120.1	121.2	121.3	119.8
Inter condenser (A) inner pressure	mbar	800.1	814.2	820.7	814.9	795.1	801.3	253.2	802.3	801.8	805.1	803.4	800.8
Inter condenser (B) inner pressure	mbar	202.3	213.5	215.3	211.4	210.7	207.8	216.9	220.3	217.5	216.2	218.9	216.3
Inter condenser (C) inner pressure	mbar	220	222.5	222.7	223	225.3	221.7	262.2	219.8	218.5	216.8	217.8	217.1
After condenser inner pressure	mbar	-0.1	2.2	1.7	1.3	1	0.8	0.9	0.4	-1.2	0.2	0	-0.3
Inter condenser (A) outlet temp.	°C	26.3	26.6	28	28.7	28.8	28.5	28.1	27.9	26.8	26.5	26.2	26
Inter condenser (B) outlet temp.	°C	38.2	38.8	36.6	36.6	36.9	36.2	36.2	38.4	38.1	37.7	38	37.4
Inter condenser (C) outlet temp.	°C	38.3	38.9	39.5	39.6	39.5	38.9	38.7	38.5	38.1	37.8	38.1	37.5
After condenser outlet temp.	°C	26.4	26.7	28.1	28.7	28.7	28.3	28	27.9	26.6	26.2	26.1	25.8
Inter condenser outlet pressure	mbar	216.5	221	218.2	219.4	220.7	217	215.8	218.1	215.6	214.3	216.2	214.1
Inter condenser outlet temp.	°C	41	41.5	41	41.1	41.2	40.6	40.4	41.1	40.8	40.3	40.6	40.1
Vacuum pump motor inboard Brg. Metal temp.	°C	39.5	42.3	46.6	47.1	44.6	43.1	42.2	41.7	39	39.6	39.5	38.5
Vacuum pump motor outboard Brg. Metal temp.	°C	36.4	39.3	44	44.4	41.9	40.2	39.3	38.8	35.6	36.3	36.5	35.3
Vacuum pump inboard Brg. Metal temp.	°C	41.3	43.9	50.4	50.5	48	43.6	44.1	44.3	42.6	43.3	42.4	42.4
Vacuum pump outboard Brg. Metal temp.	°C	37.5	39.1	40.3	39.7	36.7	37.7	38.3	38.8	39.6	39.8	39.2	38.4
Vacuum pump motor stator winding temp.	°C	49.8	52	57	58.1	55.5	53.4	51.8	52.2	48.8	49.9	49.8	48.8
Vacuum pump after condenser outlet temp.	°C	52.3	52	53.1	52.6	52.3	52.1	51.6	52.6	51.9	50.2	52.3	51.8
CCWP discharge header pressure	bar-g	2.14	2.16	2.16	2.15	2.15	2.13	2.15	2.14	2.16	2.17	2.16	2.16
CCWP discharge strainer diff. Press.	bar-g	0.248	0.245	0.24	0.233	0.236	0.224	0.233	0.23	0.234	0.232	0.227	0.236
CCW flow to cooling tower	T/H	334	335	334	335	335	331	334	335	336	335	336	335
CCW discharge inter/after condenser etc.	T/H	387.1	384.1	381.5	383.4	386.8	386.7	385.4	386.2	381.6	387.7	382.2	384.4
CCW discharge temp. to cooling tower	°C	26.9	27.4	27.8	27.9	28.2	27.5	27.4	27.2	26.8	26.4	26.7	26.2
CCW pH	pH	3.4	3.4	3.4	3.4	3.4	3.4	3.4	3.4	3.4	3.4	3.4	3.4
Instrument air receiver tank pressure	bar-a	6.9	7.1	6.9	6.9	6.9	6.9	7	7	7.1	7.1	7.2	7.1
R2 brine flow	T/H	127.1			149.8	118.3	224.4	225.3	212.7	197.4	122.5	132.2	241.7
R3 brine flow	T/H		230		70.5								
OW-703 brine flow	T/H	151.7		6.2	94.6	97.8	89.7	94.6	105.6	108.3	124		134
OW- 708 brine flow	T/H	108 _		131.3	132.7	142	136.5	163.5	130.1	126.9	126.9 _		162.7
Availability factor	%	less than 99% for the last 6 months											
Load factor	%	less than 94% for the last 6 months											
Utilisation factor	%	less than 96% for the last 5 months											
Frequency of breakdowns	_	more than 2 per months though some are caused by transmission problems											

APPENDIX IV: Plant/turbine logs after inspection

Item Description	Units	08:00	10:00	12:00	14:00	16:00	18:00	20:00	22:00	24:00:00	02:00	04:00	06:00
Unit load	MWe	35.2	35.3	35	35.4	35.3	35.3	35	35	35.1	35.2	35.1	35.2
Turbine speed	rpm	2997	3004	3005	3007	2998	3000	2999	2997	3011	3005	2989	2997
Vent station steam pressure	bar-a	4.75	4.75	4.76	4.77	4.77	4.77	4.76	4.76	4.76	4.77	4.76	4.77
In-line steam PCV opening	%	100.1	99.9	96.5	98.7	100.8	98.6	99.9	100.2	99.9	100.2	100.2	100.2
Lead vent station PCV opening	%	21.7	18	12.8	14.8	15.8	25.9	12.6	14.1	20.6	19.1	17.3	19.7
Main steam flow rate	T/H	250.4	251	250	252.1	252.3	250.4	250.6	252.4	250.4	250.6	252	251.6
Main steam temp. (scrubber inlet)	°C	153.7	153.6	153.5	153.5	153.6	153.6	153.6	153.6	153.6	153.6	153.6	153.5
Main steam press. (scrubber inlet)	bar	4.6	4.6	4.6	4.5	4.6	4.6	4.6	4.5	4.6	4.6	4.6	4.6
Steam scrubber level	mm	647	685	712	723	750	770	786	811	620	628	649	664
Steam scrubber level control v/v opening	%	0.7	0.8	0.8	0.8	0.8	0.8	0.8	0.7	0.8	0.8	0.7	0.8
Main steam temp. (turbine inlet; LH)	°C	151.1	150.9	150.8	150.8	150.9	151	151	151	151	151	151	151
Main steam temp. (turbine inlet; RH)	°C	153.5	153.3	153.8	153.3	153.4	153.4	153.4	153.4	153.5	153.5	153.4	153.4
Main steam press. (turbine inlet; LH)	bar	4.5	4.4	4.4	4.4	4.5	4.5	4.5	4.5	4.5	4.5	4.5	4.5
Main steam press. (turbine inlet; RH)	bar	4.4	4.4	4.4	4.5	4.4	4.5	4.4	4.4	4.5	4.4	4.4	4.4
Main steam coductivity	µMHO	45	50	45	60	45	44.6	44.8	44.8	44.8	45.2	55	45.4
Condenser vacuum pressure	bar-a	0.089	0.084	0.078	0.084	0.079	0.086	0.089	0.086	0.085	0.085	0.087	0.084
Auxiliary steam header pressure	bar-g	4.6	4.6	4.6	4.6	4.6	4.6	4.6	4.6	4.6	4.6	4.6	4.6
Auxiliary steam header temp.	°C	154.6	154.2	155	154	154.2	154.1	152.4	154.2	154.3	154.7	154.3	154.3
Auxiliary steam flow	T/H	14.8	14.7	14.7	14.7	14.7	14.7	14.7	14.7	14.7	14.7	14.7	14.7
Ejector steam supply header pressure	bar	4.5	4.5	4.5	4.5	4.5	4.5	4.5	4.5	4.5	4.5	4.5	4.5
Turbine gland steam pressure	bar	0.23	0.22	0.22	0.22	0.23	0.23	0.22	0.22	0.23	0.22	0.22	0.23
Turbine gland steam PCV opening	%	35.7	35.6	35.6	35.6	35.5	35.6	35.7	35.6	35.6	35.6	35.7	35.7
Lube oil pressure at cooler outlet	bar	1.73	1.75	1.75	1.75	1.74	1.73	1.74	1.74	1.74	1.74	1.74	1.75
Main oil tank level	mm	-37.3	-38.8	-37.7	-37.6	-37.3	-38.6	-38.9	-37.9	-39.3	-39.4	-39.8	-41.1
Main oil tank oil temperature	°C	60.8	61.5	61.8	62.1	62.3	61.8	61.5	61.4	61.1	61.2	61.1	60.8
Oil cooler outlet oil temperature	°C	44.2	44.8	45.2	45.2	45.5	44.9	44.6	44.6	44.3	44.3	44.2	43.9
Control oil pressure	bar	7	8.5	8	8.5	7.5	7	7.5	8	7.8	8	7.5	7.5
E/H converter (R/H) pressure	bar	2.92	3.5	4	2.32	4	4	0.66	1.11	1.87	4	0.23	0.18
E/H converter (L/H) pressure	bar	3.9	1.86	2.69	3.21	3.06	4	1.63	3.76	3.2	1.53	1.73	1.64
No. 1 bearing metal temperature	°C	69.4	69.8	70.1	70.3	70.4	69.8	69.7	69.7	69.5	69.4	69.5	69.2
Thrust bearing metal temp. (Gov. side)	°C	60.5	60.5	60.8	60.9	61	60.4	60.3	60.3	60.1	60.1	60.1	59.8
Thrust bearing metal temp. (Gen. side)	°C	51.5	51.4	52.4	52.6	52.7	52.2	51.9	52	51.8	51.7	51.8	51.4
No. 2 bearing metal temperature	°C	66.1	67.6	66.8	67	67.1	66.6	66.4	66.4	66.3	66.3	66.3	66.1
No. 3 bearing metal temperature	°C	68	68.6	68.6	68.8	69.1	68.4	68.3	68.4	68.3	68.2	68.3	68
No. 4 bearing metal temperature	°C	63.8	64	64.4	64.5	64.7	64.2	63.9	64	63.8	63.8	63.8	63.5
No. 1 bearing vibration (X/Y)	µm	12:13	12:13	12:13	12:13	12:13	12:13	12:13	12:13	12:13	12:13	12:13	12:13
No. 2 bearing vibration (X/Y)	µm	15:15	14:16	15:15	15:15	15:16	14:16	15:16	14:15	15:16	14:15	14:16	15:16
No. 3 bearing vibration (X/Y)	µm	21:17	22:17	22:17	22:18	22:18	23:18	23:19	22:18	23:18	22:18	23:19	22:18
No. 4 bearing vibration (X/Y)	µm	19:33	19:33	19:35	19:32	19:13	20:33	20:33	20:33	19:34	20:34	20:34	20:34
Turbine rotor position	mm	-0.14	-0.14	-0.14	-0.14	-0.14	-0.14	-0.14	-0.14	-0.14	-0.14	-0.14	-0.14
Turbine differential expansion	mm	1.53	1.52	1.52	1.5	1.48	1.49	1.49	1.49	1.52	1.52	1.52	1.53
Governing valve (LH) opening	%	78	88	87	84.1	81.5	81.5	78.5	74.1	78.1	74.1	78	80.2
Governing valve (RH) opening	%	81.6	89.8	86.2	83.1	80.4	75.8	78.5	73.6	80.2	79.8	75.8	76.7
Turbine steam chest pressure	bar-a	3.65	3.7	3.65	3.7	3.62	3.64	3.65	3.66	3.65	3.67	3.67	3.66
Turbine exhaust steam pressure	bar-a	0.089	0.09	0.091	0.092	0.094	0.09	0.089	0.089	0.087	0.086	0.088	0.085
Turbine exhaust steam temperature	°C	44.7	45.3	45.6	45.9	46	45.2	45.1	45	44.6	44.3	44.5	44
Condenser level	mm	1404	1246	1240	1403	1478	1434	1335	1308	1390	1354	1351	1404
Hot well water temperature	°C	42.3	41.8	42	42.6	42.3	41.7	41.5	41.6	41.8	41.2	42.4	41.8
Circulating water FV (gas cooler)	%	35.4	35.3	35.3	35.3	35.3	35.3	35.3	35.3	35.3	35.4	35.3	35.3
Circulating water FV (condenser)	%	62.8	62.8	62.7	62.7	62.8	62.8	62.7	62.8	62.8	62.8	62.7	62.8
Hot well pump No. 1 vibration (X/Y)	mm/s	2.3:3.5	2.3:3.4	2.1:4.0	2.1:3.6	2.0:3.5	2.2:3.4	2.4:3.6	2.3:4.5	2.2:3.9	2.2:3.7	2.2:4.0	2.5:3.8
Hotwell pump 1 stator winding temp.	°C	127.3	128.3	133.1	134	133.9	131	130.4	129.7	127.1	126.4	126.1	125.6
Hotwell pump 1 motor inner bearing metal temp.	°C	51.5	52.6	57.3	58.2	57.2	54.6	54.3	53.8	50.7	49.8	50.3	48.8
Hotwell pump 1 motor outer bearing metal temp.	°C	79.5	80.5	85.2	86.2	85.6	83.1	82.3	82	79	78.3	78.7	77.5
Hotwell pump 1 recirculation v/v opening	%	0.4	0.4	0.4	0.4	0.4	0.4	0.4	0.4	0.4	0.4	0.4	0.4
Hotwell pump 1 discharge v/v opening	%	63.3	58.8	57.6	57.8	59.5	61.2	61.5	58.2	62.5	58.5	58.1	60.3
Hot well pump No. 2 vibration (X/Y)	mm/s	1.8:2.0	1.8:1.7	1.5:1.6	1.5:1.5	1.6:1.7	1.6:1.7	1.8:1.7	1.9:1.6	1.8:1.6	1.5:1.7	1.6:2.0	1.9:2.2
Hotwell pump 2 stator winding temp.	°C	125	125.7	130.1	132.7	130.3	129.2	127.7	127.7	126.4	124.5	124.5	123.5
Hotwell pump 2 motor inner bearing metal temp.	°C	48.6	49.7	54.7	55.4	53.7	51.7	50.9	50.4	50.1	48.2	47.7	46.2
Hotwell pump 2 motor outer bearing metal temp.	°C	69.2	70.5	75.9	76.8	75.4	73.2	72.2	71.8	71.1	69.1	69	67.5
Hotwell pump 2 recirculation v/v opening	%	0.8	0.8	0.9	0.9	0.8	0.8	0.8	0.8	0.8	0.8	0.8	0.8
Hotwell pump 2 discharge v/v opening	%	64.5	59	62.1	59.3	61.1	60.9	61.5	62.2	61.5	62.3	62.2	61.6
Hotwell discharge header pressure	bar	1.8	1.7	1.7	1.7	1.7	1.7	1.7	1.7	1.7	1.7	1.7	1.7
Hotwell discharge header temperature	°C	41.6	42.2	42.8	43.1	43.2	42.3	42.1	42	41.6	41.2	41.5	40.9
C/T to condenser water flow rate	T/H	7461	6894	7377	7438	7411	7429	7558	7188	7600	7282	7161	6729
C/T basin upstream water level	mm	777.3	758.7	717.3	714.6	759.5	768	730.2	711.3	766.8	760.2	748	742.1
C/T basin downstream water level	mm	727.4	710.5	665.5	661.7	707	715.8	676.8	659	713.3	705.9	694.2	685.5
C/T fan 1 motor winding temp.	°C	74.5	76.7	80.7	81.5	78.8	77.2	76.5	76.3	73.4	74.5	74.9	73.7
C/T fan 2 motor winding temp.	°C	71.6	73	76.7	78.5	77.6	74.5	73.4	73.1	70	70.3	70.7	69.6
C/T fan 3 motor winding temp.	°C	71.4	73.5	77.8	79.2	77.5	74.3	73.4	73.1	69.5	70.4	70.4	69.4
C/T fan 4 motor winding temp.	°C	71.9	73.6	77.2	79.2	78.4	75.2	74.5	74.2	70.7	71.1	71.4	70.3
C/T fan 1 gearbox vibration	mm/s	11	11.9	13.9	10	8.6	8.9	12	9.5	11.3	12.9	8	13.2
C/T fan 2 gearbox vibration	mm/s	14.4	13.4	12.3	10.8	12.2	11	11.7	10.7	13.8	12.6	12	14.2
C/T fan 3 gearbox vibration	mm/s	11.4	13.8	11.5	11.7	9.2	11.9	11.2	13.6	11	14.5	9.4	9.8
C/T fan 4 gearbox vibration	mm/s	14.5	12.3	10.7	11	10.8	13.7	13.7	10.6	15.2	14.5	13.4	13.1
Cond. Reijection pump disch. Header pressure	bara	12.7	12.8	12.7	1.8	1.8	12.7	12.7	12.8	1.8	12.8	12.8	12.8
Cond. Reinjection pump discharge flowrate	T/H	67.9	69.2	68.4			68	68.4	68.4		68.7	68.5	68.4
Cond. Reinjection pump discharge pH	pH	7.1	7.0	6.8	6.9	7.0	7.0	6.9	6.8	6.9	7.0	6.8	6.9
Inter-condenser inlet gas header temp.	°C	29.8	33.5	33.6	33.8	32.6	32.9	29.7	30.8	31.5	30.5	31.6	30.1
Inter-condenser inlet gas header press.	mbar	121.5	126.3	141.6	141.7	141.8	137.1	145.2	123	120.1	121.2	121.3	119.8
Inter condenser (A) inner pressure	mbar	800.6	814.7	820.9	814.7	798.5	801.6	821.6	803.5	802.6	805.1	805.3	800.8
Inter condenser (B) inner pressure	mbar	215.7	213.5	215.7	211.4	210.7	207.8	216.9	220.6	217.5	216.8	218.9	218.3
Inter condenser (C) inner pressure	mbar	220.3	221.5	223.7	223.4	224.5	221.7	222.5	219.8	218.5	216.8	217.8	217.6
After condenser inner pressure	mbar	-0.1	2.2	1.7	1.3	1	0.8	0.9	0.4	-1.2	0.2	0	-0.3
Inter condenser (A) outlet temp.	°C	26.3	26.6	28	28.7	28.8	28.5	28.1	27.9	26.8	26.5	26.2	26.3
Inter condenser (B) outlet temp.	°C	38.3	38.6	36.7	36.5	36.8	36.4	36.1	38.5	38.2	37.8	38.4	37.6
Inter condenser (C) outlet temp.	°C	38.5	38.9	39.5	39.8	39.5	38.6	38.7	38.4	38.1	37.6	38.5	37.5
After condenser outlet temp.	°C	26.4	26.7	28.1	28.7	28.7	28.3	28	27.9	26.6	26.2	26.1	25.8
Inter condenser outlet pressure	mbar	216.5	221	218.2	219.4	220.7	217	215.8	218.1	215.6	214.3	216.2	214.1
Inter condenser outlet temp.	°C	41	41.5	41	41.1	41.2	40.6	40.4	41.1	40.8	40.3	40.6	40.1
Vacuum pump motor inboard Brg. Metal temp.	°C	39.5	42.3	46.6	47.1	44.6	43.1	42.2	41.7	39	39.6	39.5	38.5
Vacuum pump motor outboard Brg. Metal temp.	°C	36.4	39.3	44	44.4	41.9	40.2	39.3	38.8	35.6	36.3	36.5	35.3
Vacuum pump inboard Brg. Metal temp.	°C	41.3	43.9	50.4	50.5	48	43.6	44.1	44.3	42.6	43.3	42.4	42.4
Vacuum pump outboard Brg. Metal temp.	°C	37.5	39.1	40.3	39.7	36.7	37.7	38.3	38.8	39.6	39.8	39.2	38.4
Vacuum pump motor stator winding temp.	°C	49.8	52	57	58.1	55.5	53.4	51.8	52.2	48.8	49.9	49.8	48.8
Vacuum pump after condenser outlet temp.	°C	52.3	52	53.1	52.6	52.3	52.1	51.6	52.6	51.9	50.2	52.3	51.8
CCWP discharge header pressure	bar-g	2.15	2.16	2.14	2.15	2.16	2.13	2.16	2.15	2.16	2.17	2.16	2.18
CCWP discharge strainer diff. Press.	bar-g	0.248	0.245	0.240	0.233	0.236	0.224	0.233	0.230	0.234	0.232	0.227	0.236
CCW flow to cooling tower	T/H	336	335	334	333	335	332	333	335	332	334	336	335
CCW discharge inter/after condenser etc.	T/H	387.1	385.3	387.7	387.8	386.8	391.1	384.6	386.6	383.3	389.5	381.3	384
CCW discharge temp. to cooling tower	°C	26.8	27.8	27.8	27.2	27.2	27.5	27.2	27.2	26.2	25.9	24.8	26.1
CCW pH	pH	3.4	3.3	3.4	3.3	3.3	3.4	3.3	3.4	3.2	3.3	3.3	3.4
Instrument air receiver tank pressure	bar-a	6.9	7.1	6.9	6.9	6.9	6.9	7	7	7.1	7.1	7.2	7.1
R2 brine flow	T/H	_	220.1	_	190.8	_	187.4	161.5	116.6	_	_	_	87.3
R3 brine flow	T/H	_	_	_	337.9	_	167.2	_	_	_	119.3	_	_
OW-703 brine flow	T/H	105.3	98.8	_	92.9	_	99.7	107.3	142.3	_	_	96.9	114
OW- 708 brine flow	T/H	_	_	187	100.7	_	102.3	204.6	137	_	187.3	178.5	107.7
Availability factor	%	Its 99% has been observed to improve											
Load factor	%	Load factor has improved to more than 99% for the next 6 months											
Utilisation factor	%	Utilisation factor has improved to more than 98% in the next 6 months											
Frequency of breakdowns	_	On average its 2 per month and still some breakdown are caused by transmission problems											